

POSTERS

VARIABLE ENERGY (6-15) MeV ELECTRON LINAC FOR MEDICAL APPLICATIONS

J. Bigolas, S. Getka, A. Kucharczyk, S. Kulinski, W. Maciszewski, M. Pachan, E. Plawski
The A. Soltan Institute for Nuclear Studies, Otwock-Swierk, Poland

E. Jankowski, L. Kotulski, J. Pracz
The A. Soltan Institute for Nuclear Studies, Establishment for Nuclear Equipment,
Otwock-Swierk, Poland

Abstract. A variable energy linac is described and the most important parameters are given.

1. INTRODUCTION

During past 25 years in our Institute a series of medical electron linear accelerators (linac) have been developed and produced: 4 MeV LIMEX and COLINE and 10 MeV NEPTUN. These accelerators were principally single X-ray energy machines. The necessity of more universal multi-energy therapeutic accelerators was signalled by oncological hospitals. In response the State Committee for Scientific Research put the task to develop such an accelerator in The Soltan Institute for Nuclear Studies, where the know-how of S-band electron linac techniques and technology is mastered since a long time. As a result the new variable energy medical electron linear accelerator was constructed with the following parameters: electron energies 6, 9, 12, 15 MeV at dose rate up to 4 Gy/min/m; electron energies for X photon generation 6 and 15 MeV at X-ray dose up to 3 Gy/min/m.

2. THERAPEUTIC LINAC REQUIREMENTS

The basic parameters of the new medical linear electron accelerator are the following:

Electron energy	-	6, 9, 12, 15 MeV
at dose rate	-	up to 4 Gy/min/m.
Electron energy for X photons generation	-	6, 15 MeV
at dose rate	-	up to 3 Gy/min/m.
Distance source-isocentre	-	1 m
Electron beam diameter on the e ⁻ /X target	-	2 mm
Irradiation field area:		
For electrons	-	from 2x2 cm to 30x30 cm
For photons	-	from 2x2 cm to 40x40 cm

Computerized steering for 3 modes of operation:
Therapy, maintenance and investigation & measurements.

3. PRINCIPAL PARTS OF THE ACCELERATOR

3.1. Electron Sources

In up to now medical electron accelerators built in Poland: Neptun, Limex, Coline the source of electrons was diode gun with thermionic cathode made of tungsten.

In this gun with anode voltage of about $V_a=40\text{kV}$, electron current above 0.5 A at 5 μs pulse length was obtained. The parameters of the gun were optimised with the aid of Hermannsfeldt EGUN code. The advantage of this type of guns is their simple construction and, especially,

when used in linacs having magnetron as RF power supply, since then the high voltage is common for magnetron and the gun. For the new 6/15 medical accelerator the final solution will be a triode gun. For that purpose spherical cathode - grid assembly was bought with the following nominal data claimed by the producer: $grid_{cut\ off} = -60V$, $grid_{drive} = +60V$ for 1A at $U_a=12kV$; $grid\ current=12\%I_c$, $grid_{load} = 1W_{max}$; heater 6.3V/2.0A; Pulse width 100 μ sec max, duty cycle 0.04 max is allowed. The cathode material is of dispenser type. The vacuum conditions for this type of cathode are rather severe (better than 5×10^{-7} Torr). The advantage of triode over diode gun is independent regulation of gun current and energy at much lower heater power and lower anode voltage. The gun dimensions are reduced at least twice. The measuring, high vacuum stand equipped with the wire scanners was built to measure and verify the calculated optical parameters. The first measured results are shown in Fig. 1 and the geometry of the gun with beam trajectories is presented in Fig. 2.

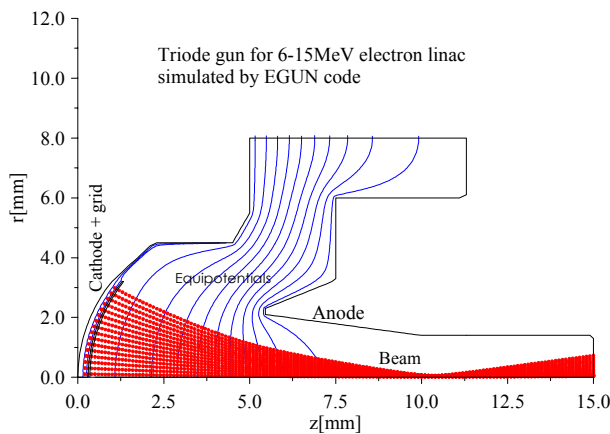


Fig.1 Triode GUN. $U_a=12kV$, $U_g=60V$, $I=0.4A$.

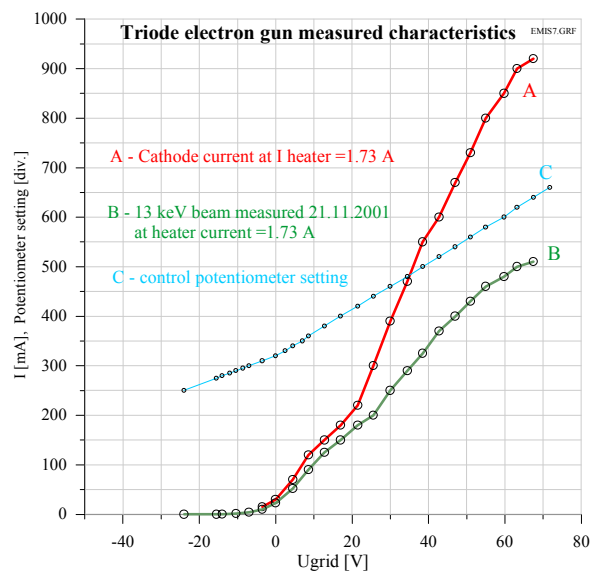


Fig. 2 Measured gun characteristics at pulse length 10 μ sec.

3.2. Accelerating Structure

The designed and constructed SW S-band accelerating structure is operating at 2998.5 MHz. It is biperiodic $\pi/2$ mode, on axis coupled structure and is composed of 29 accelerating cells. To get good phase acceptance and cover large electron energy variation from 6 to 15 MeV, the first few cells have graded beta between 0.65 and 0.95. Additionally the value of electron gun energy is adjusted for each of output energies. To fix the RF parameters of the structure, the SUPERFISH code was used [1]. The focusing solenoid of special type and system of correction coils surrounding the structure, guide the beam on axis.

The longitudinal and transverse beam dynamics in 6-15 MeV linac were studied using the codes developed for the purpose in our Laboratory [2,3]. Results of these calculations are shown in Figs 3-6. Methods of design and construction of the accelerator were presented in [4,5].

The dependence of beam output energy and transverse dimension on the RF input phase at optimal values of magnetic field of solenoid are shown in Fig.1 and Fig.2. To minimize the magnetic field on gun cathode, the bucking coil is added at input of solenoid. This substantially improves the action of iron magnetic shield placed inside the input side of accelerating structure.

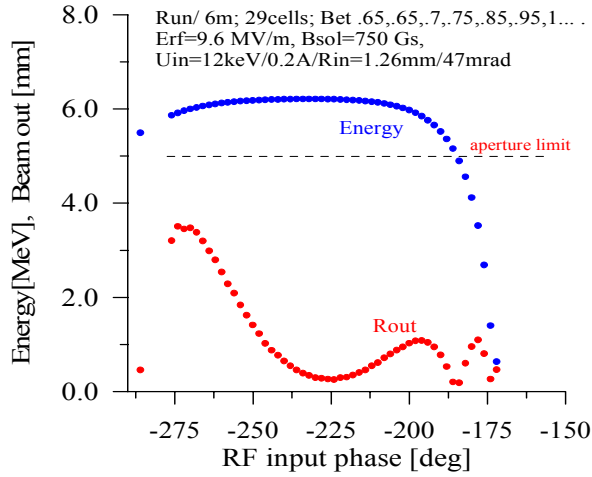


Fig. 3 Output energy and beam size at RF field level corresponding to 6 MeV energy.

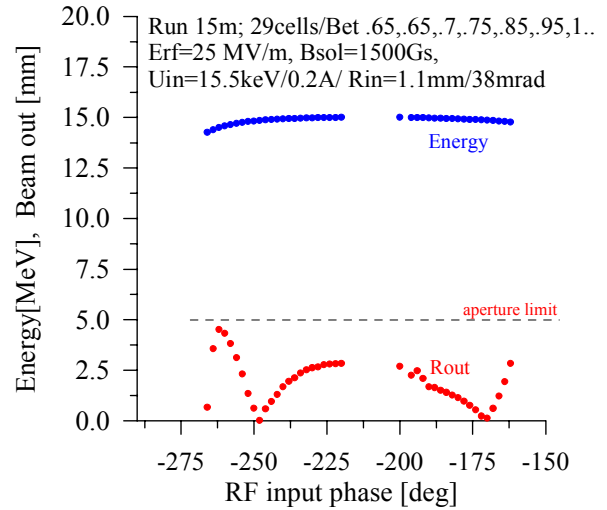


Fig. 5 Output energy and radial beam size at RF field corresponding to 15 MeV.

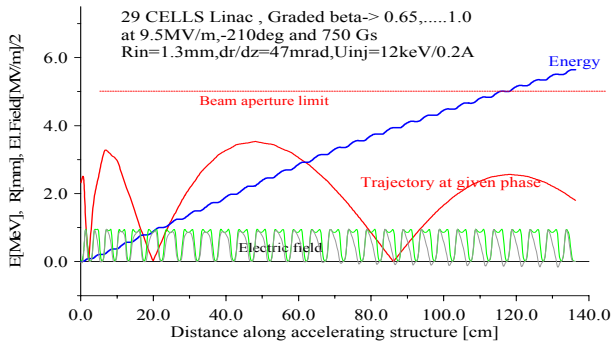


Fig. 4 Acceleration process at 9.5 MV/m peak electric field and -210° rf input phase $E_{out}=6\text{MeV}$.

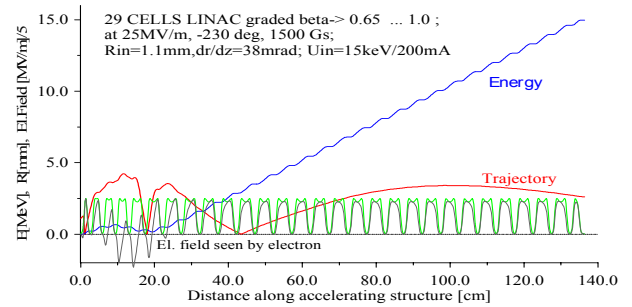


Fig. 6 Acceleration process to 15 MeV at 25MV/m peak electric field and -230° rf input phase.

3.3. Collimator

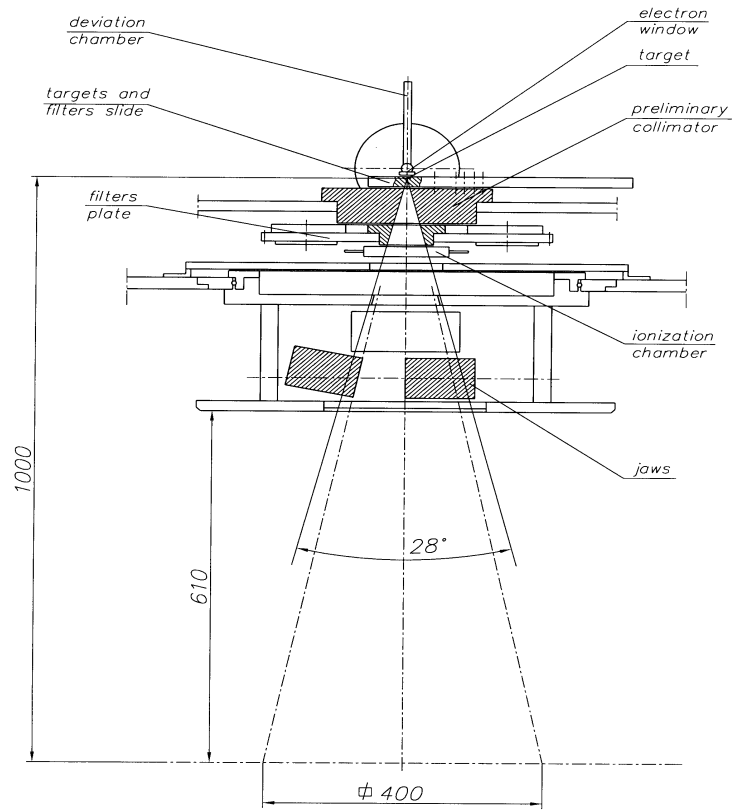
To guarantee two photon energies 6 and 15 MeV a special target strip translating in air below the electron window of the accelerating structure was applied.

Additionally, the target strip accommodates upper electron scattering filters for energies 6, 9, 12 and 15 MeV.

The target strip is slide-mounted in the fixed collimator.

The filter plate with attached collimators is located under the fixed collimator. These collimators are equipped with two equalising filters for photons, four lower filters for electron scattering, and new system of optical simulation. The distance between the upper and the lower filters amounts to about 100 mm.

A double ionisation chamber is located under the filter plate. The ionisation chamber is mounted in a tilting mechanism allowing for rotation of the filter plate in one direction.



Collimator scheme

Fig. 7 Scheme of Collimator.

FUNCTIONAL AND BLOCK DIAGRAM OF ACCELERATOR 6/15

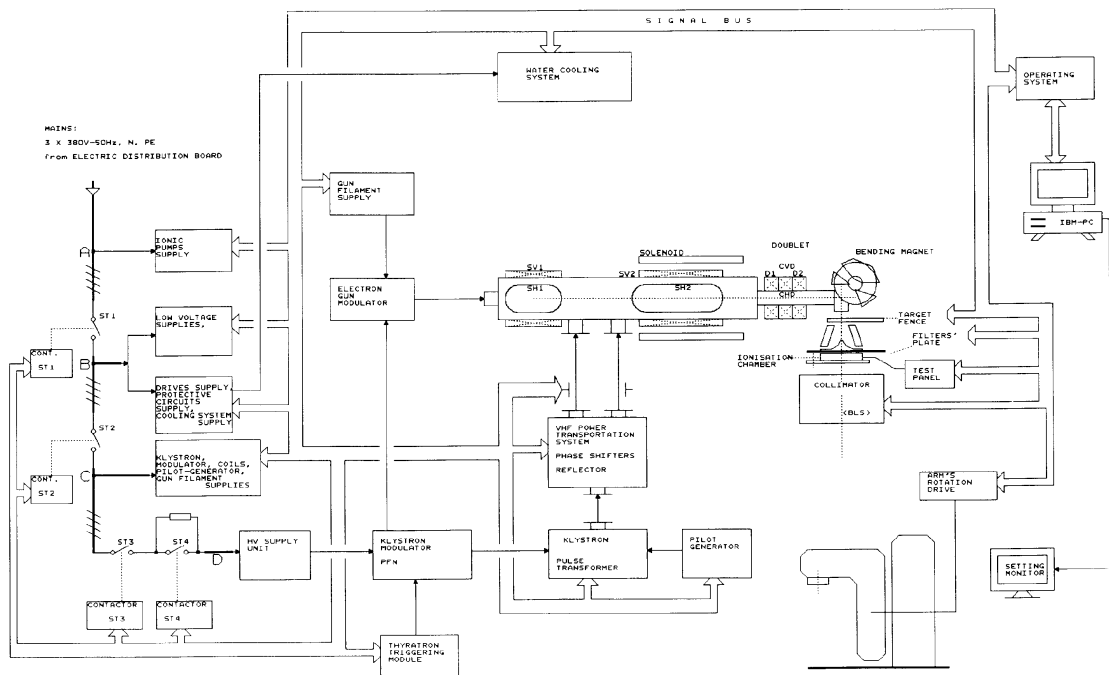


Fig. 8 Functional and block diagram of accelerator 6/15.

The lower part of the collimator is formed by a system of mobile diaphragms (jaws). The adopted design solutions of the drives and position reproduction allow for precise, asymmetric motion of the two pairs of jaws with a possibility of crossing the zero position. The design of the final version will allow for additional use of the upper pair of jaws as a dynamic wedge.

Due to the use of sintered tungsten of density 18g/cm^3 , as shielding material for collimators and jaws, the vertical size of the collimator has been reduced. The attained overall dimensions make it possible to mount an additional multi-leaf collimator and a number of accessories under the present collimator.

The design calculations of the size of fixed collimator, the collimators in filter plate, and jaws takes into account the contemporary tendencies as regards radiological safety. The whole design of the collimator of 6/15 accelerator conforms to provisions of IEC Standard.

The collimator scheme is shown in Fig. 7.

Most of the principal elements of the accelerator are already produced and present the process of accelerator assembling and testing is going on.

Functional and block diagram of accelerator 6/15 is presented in Fig. 8.

REFERENCES

- [1] J.H.BILLEN, L.M.YOUNG, "Poisson Superfish", LA-UR-96-1834 Rep., Los Alamos, Nov.1996
- [2] S. KULINSKI, Program LISA, To be published .
- [3] E. PLAWSKI, "ELINAC code", Inst. For Nuclear Studies, Internal Rep. To be published.
- [5] Annual Report 1999 of Institute for Nuclear Studies p.172
- [6] Annual Report 2000 of Institute for Nuclear Studies

ACCELERATED ELECTRON BEAMS FOR PRODUCTION OF HEAT SHRINKABLE POLYMERIC PRODUCTS AND PTFE WASTES RECOVERY

Gh. MARIN

SC ICPE Electrostatica SA,
Bucharest, Romania

M. MARCUTA

SC ICPE Electrostatica SA,
Bucharest, Romania

S. JIPA

“Valahia” University,
Targoviste, Romania

Abstract. A pilot station for radiation curing of polymeric materials by electron beams is described.

Radiation curing, i.e. curing under the action of ionizing radiation (predominantly electron beams) is one of the most important areas of radiation processing.

There are many practical applications of electron beam processing. Our research activity was focused on two of them:

- radiation cross-linking of polymeric materials;
- recovery of PTFE wastes.

For these purposes we have used the pilot station with the following modules (figures 1a and 1b): an industrial electron accelerator ILU-6 with 2.5 MeV electron energy and 40kW beam power, equipment for the transport of materials under the electron beam, a technologic line with typical equipment for the expansion process and testing laboratory.

It is generally accepted that the result of polymer cross-linking process induced by irradiation is a three-dimensional network, where each polymer chain is linked to another one.

This structural change induces beneficial changes in mechanical and chemical properties and thermal stability of polymer.

In order to settle the radiation dose experimental measurements were done on different materials: polyethylene, polyethylene antioxidative stabilized and flame retardant polymeric compound. these samples had different wall thickness.

The material investigated had to provide some special properties:

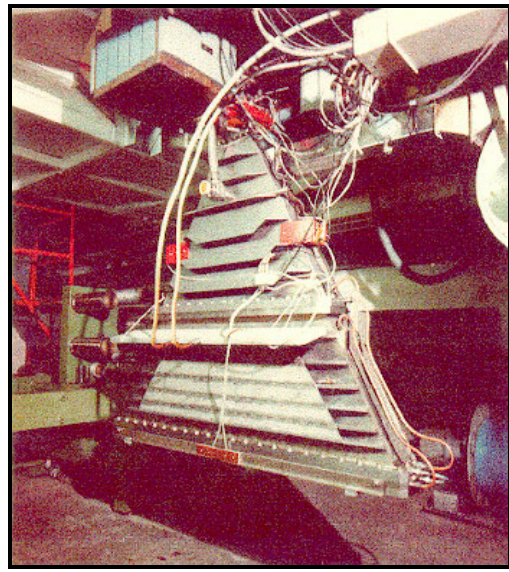
- a large shrinkage range;
- tensile strength and elongation at break no less than a minimum value, (fig 3);
- heat resistance to allow a high temperature classification.

Cross-linked polymeric materials were used to obtain heat shrinkable products: tubes, sheds.

The heat shrinkable manufacturing process is formulated in figure 5.



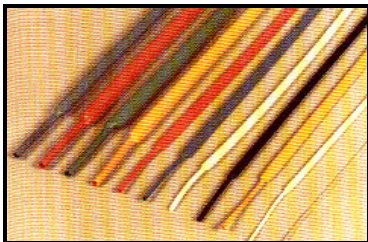
a. Upper part



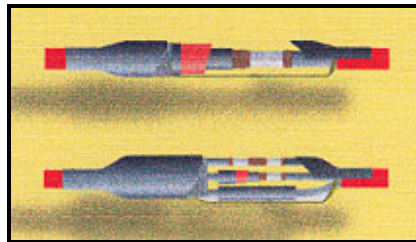
b. Lower part

Figure 1. General view of the ILU-6M accelerator.

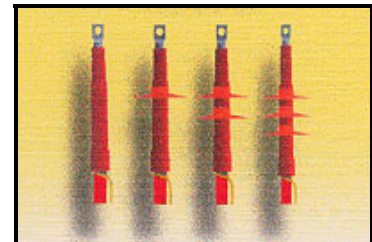
Because of their excellent features heat shrinkable products are suitable for a wide variety of applications such as electrical wire and cable insulation, voltage power cable joints, and voltage power cable indoor and outdoor terminations (figures 2a, 2b and 2c).



a. electrical wire and cable insulation



b. voltage power cable joints



c. voltage power cable indoor and outdoor terminations

Figure 2. Heat shrinkable products – main industrial application of ILU-6M electron accelerator.

The main-chain degradation of polytetrafluoroethylene (PTFE) wastes was another important technology where the electron beam curing was used.

Teflon is known as one of the most inert polymer towards heat, solvents and most corrosive chemicals. Moreover it has excellent grease properties, wear out resistance, electrical and mechanical properties.

In contrast it is extremely sensitive to radiation and suffers marked damage in its mechanical strength after very low radiation doses.

The researches were carried on to provide:

- the irradiation of samples with a radiation dose in the range of 0,3-62,4 kGy;
- elongation at break and tensile strength;
- weight loss.

The experimental results settled the irradiation dose for a high degradation of the polymer. The PTFE wastes became brittle and have been crumbled into powder with a special device. After the milling of the PTFE wastes, granulometric measurements were carried out and the variation of the density with the milling time was determinate for different irradiation doses, (fig 4).

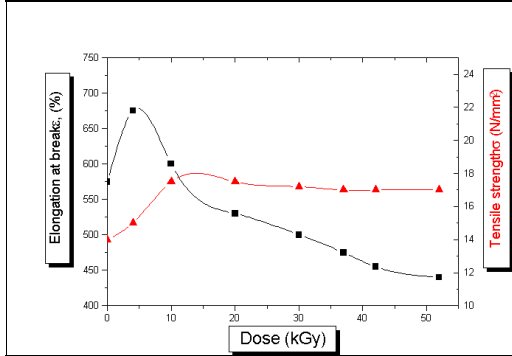


Fig. 3. Influence of dose on the elongation at break and tensile strength.

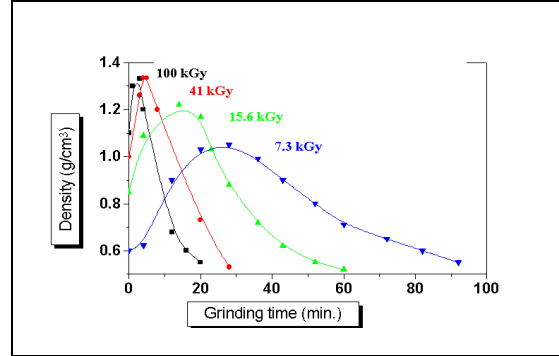


Fig. 4. Variation of density with the willing time subjected to various doses.

On the other hand, because of the gases removal (CO , CO_2 , COF_2), during the PTFE radiation curing, the dependence irradiation dose-weight loss was determined.

Figure 6 shows the technological line for PTFE micro powders manufacture.

Because of the main structural changes of the irradiated PTFE wastes, the powder was used to obtain semi-finished electrical and mechanical products, filler for special greases, metallic pieces covering, s.o.

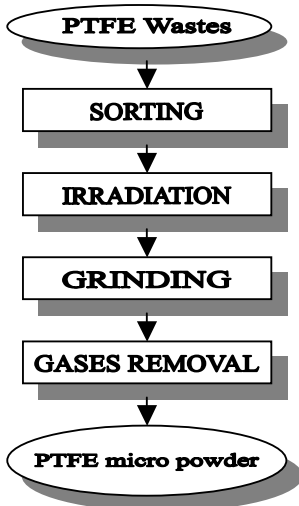


Figure 5. Heat shrinkable products manufacturing process.

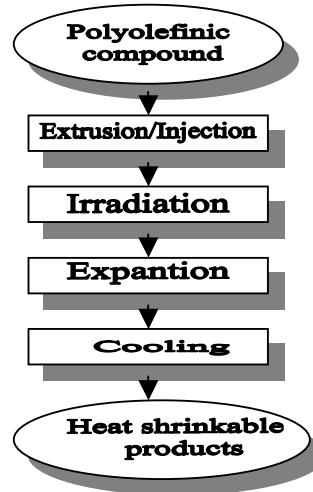


Figure 6. Technological line for PTFE micro powder manufacture.

REFERENCES

- 1) MACHI, Sueo., "Prospects of Radiation Technology for Industrial and Environmental Protection" Interregional Training Course, Warsaw, Poland, Oct 1997
- 2) ZYBALL, A., "Irradiation Cross-linking of Polyethylene in the Presence of Polymerizable Additives", *Kunststoffe, German Plastics* 67 (1977) 8 p. 461.
- 3) MARIN, Gh., a.o., "Pilot Station for Materials processing by Irradiation with Accelerated Electrons" (Proc. RadTech Asia'95 Conference), Guilin, China, (1995) 481-486.

UTILIZATION OF DNA COMET ASSAY AND HALF EMBRYO TEST TO IDENTIFY IRRADIATED LENTIL

M.F. ROMANELLI, A.L.C.H. VILLAVICENCIO*

Centro de Tecnologia das Radiações – CTRD,

São Paulo, Brazil

Abstract. Insect infestation cause extensive damage in stored grains. Over the last few decades some countries adopted food irradiation as a safe food process. Irradiation has been shown to be an effective pest control method for these commodities and a good alternative to prohibited methyl bromide. As screening methods to identify irradiated lentils, processed by e-beam as a food treatment to disinfestation, the DNA Comet Assay and Half Embryo tests were performed. The methodologies used in this work are based upon biological changes that occur in Brazilian lentils. DNA fragmentation was studied using single cell gel electrophoresis. Irradiated cells produced typical comets with DNA fragments migrating towards the anode. DNA of non-irradiated cells exhibited a limited migration. The half-embryo test is based on the inhibition of shooting in seeds or grains due to irradiation. It is characterised by its easy detection and sensitivity. Irradiated half-embryo showed markedly reduced root grows and almost totally retarded shoot elongation. Differences between irradiated and non-irradiated half-embryo could be observed.

1. INTRODUCTION

Legumes make an important contribution to human nutrition on a world-wide basis. Insect infestation cause extensive damage to stored grains. Over the last few decades some countries adopted food irradiation as a safe food process. Radiation's processing improves hygienic quality and extends shelf life of various food products, such as grains, dried fish, and dried fruits and legumes [1].

The use of radiation treatment to reduce the microbial population and thereby extend the shelf life in legumes has been reported in many papers. Irradiation has been shown to be an effective pest control method for these commodities and a good alternative to prohibited methyl bromide.

Radiation disinfestation can facilitate trade in foods that often harbour insect pests of quarantine importance. Irradiation is a suitable method for grain preservation because it can effectively destroy moulds and insects without any pollution. Although the wholesomeness of irradiated food is no longer a question there is a need for irradiation control in the international trade of foods, in order to enhance the consumer confidence in the regulation. To promote the commercial application of this technology, many identification methods based on the changes occurred in irradiated foods have been developed [2].

*Corresponding author. **IPEN-CNEN/SP, Centro de Tecnologia das Radiações - CTRD**

Travessa R. Nº 400. Cidade Universitária. CEP: 05508-910, São Paulo, Brazil.

Fax: +55-11-3816-9186

E-mail address: villavic@net.ipen.br (Anna Villavicencio).

As screening methods to identify irradiated lentils, processed by e-beam as a food treatment to disinfestation, the DNA Comet Assay and Half Embryo tests were performed. The methodologies used in this work are based upon biological changes that occur in Brazilian lentils. Irradiated cells should be identified since extensive DNA damage will lead to migration of DNA fragments out of the cells, producing typical comet tails [3], and germination test is a valuable biological method for the identification of irradiated foods [2].

2. MATERIAL AND METHODS

Samples - Lentils were bought in a local market in São Paulo.

Irradiation - The samples were irradiated in an electron beam accelerator facility of Radiation Dynamics Inc., USA (E= 1,5 MeV, I=25mA). The irradiation doses were 0,7; 1,4 and 3,0 kGy at dry conditions. The thickness of samples was less than 0,5 cm.

DNA Comet Assay - A sensitive technique to detect DNA fragmentation is the microgel electrophoresis of single cells or nuclei, also called “comet assay”. Since the large molecule of DNA is an easy target for ionising radiation, changes in DNA offer potential as a detection method. The DNA Comet Assay was performed as described by Cerda *et al.* (1997) [3]. The silver stained slides were evaluated in a standard transmission microscope. It is restricted to foods that have not been subjected to heat or other treatments, which also cause DNA fragmentation. Lentil samples were crushed with a mortar and pestle and was transferred to 3ml ice-cold PBS. This suspension was stirred for 5 minutes and filtered. 100µl cell suspension was mixed with 500µl of low-melting agarose (0,8% in PBS). 100µl of this mixture was spread on pre-coated slides. The slides were immersed in lysis buffer (0,045M TBE, pH 8.4, containing 2,5% SDS) for 15 minutes. Electrophoresis was carried out using the same TBE buffer, but devoid of SDS, at a potential of 2V/cm for 2 minutes. Silver staining was carried out for 1 hour following fixing. Duplicate measurements for each sample were carried out and 100 cells were counted for each dose level. The migration patterns of DNA was evaluated with a standard microscope.

Half Embryo Test - The half-embryo test was carried out as described by Kawamura *et al.* (1998) [4]. Germination tests were carried out in the irradiated and non-irradiated dry lentils, which allows observing characteristically variations on the shoots and roots. The half-embryo test is based on the inhibition of shooting in seeds or grains due to irradiation. It is characterised by its easy detection and sensitivity. The shoots and roots were observed during 5 days of culturing period under specified conditions. The difference observed in this variety was analysed only after irradiation treatment at room temperature.

3. RESULTS AND DISCUSSION

The present work results from the need for a simple, fast and reliable comet assay for identification irradiated food.

In the DNA Comet Assay non-irradiated cells of the lentils exhibited only limited DNA migration out of the cells (figure 1). The DNA migration out of the irradiated cells producing typical comets tails (figure 2, 3 and 4).

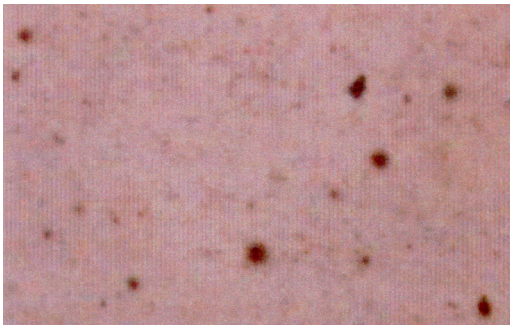


Figure 1: Non-irradiated cells of lentil.

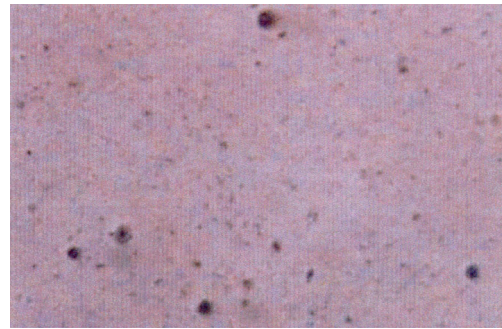


Figure 2: Irradiated cells migration of lentil, 0,7 kGy.

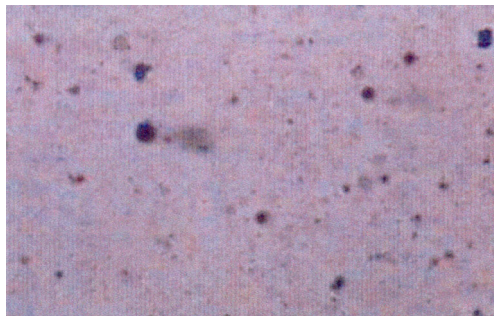


Figure 3: Irradiated cells migration of lentil, 1,4 kGy.

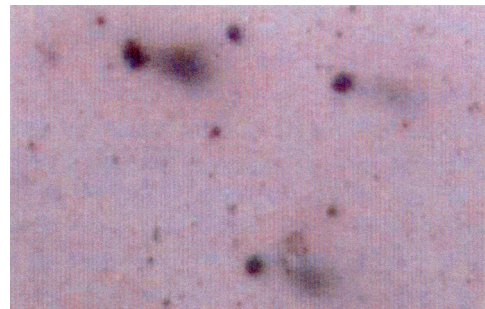


Figure 4: Irradiated cells migration of lentil, 3,0 kGy

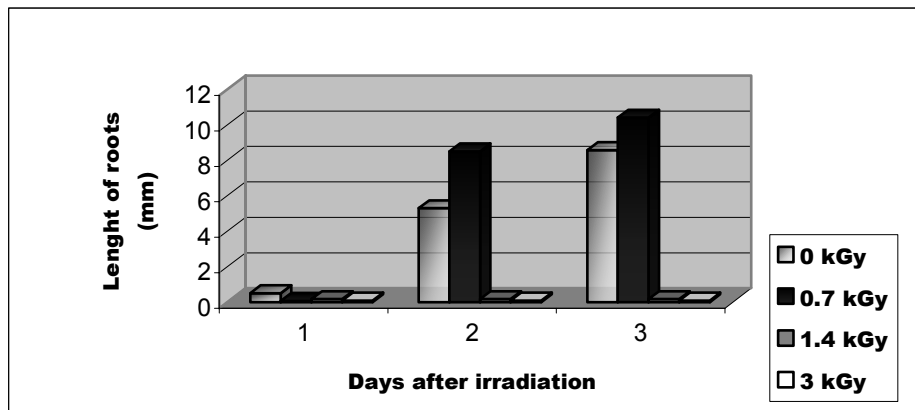


Figure 5: Germination comparison between non- irradiated and irradiated roots of lentils.

Previous experiments with irradiated food using the DNA Comet Assay have shown that this method is a rapid and simple technique to detect the radiation treatment in both animal food [5] as well as in plant material [6]. Khan & Delincée, 1998 [7], used DNA comet assay to identify irradiated lentils in a gamma source with 1 kGy. Villavicencio *et al.*, 1997 [8], showed some DNA fragmentation in irradiated beans.

The germination of lentils was studied, to determine the influence of radiation in roots and shoots elongation after incubation. Differences between irradiated and non-irradiated half-embryo could be observed.

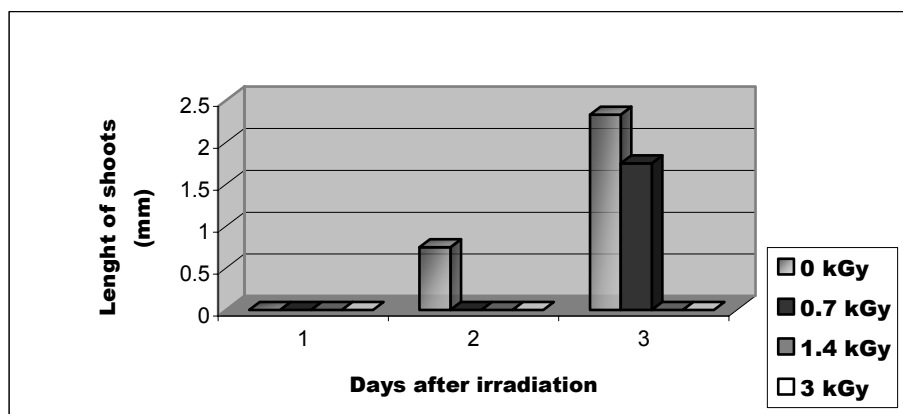


Figure 6: Germination comparison between non- irradiated and irradiated shoots of lentils.

It was observed that the damage by irradiation in roots and shoots has some especial characteristics. With the dose of 0,7 kGy the germination rate was not affected, but the growth was inhibited. With the doses 1,4 and 3,0 kGy shoots and roots were very short and the growth of them was seriously inhibited. Figure 5 show the root length (mm) and figure 6 show the shoot length (mm). Irradiated half-embryo showed markedly reduce roots grows almost totally retarded shoot elongation.

Kawamura *et al*, 1992 [9], studied the germination of wheat and concluded that the critical dose that inhibits root growth varies from 0,15 to 0,5 kGy. Fifield *et al*. 1967 [10], showed that the germination of wheat was unaffected by radiation dose of 0,1 and 0,25 kGy, whereas, at 0,5 kGy or more germination was substantially reduced. Villavicencio *et al.*, 1997 [11], identifies by germination two kinds of irradiated beans. Half-embryo tests with lemon and orange seeds were also proposed by Kawamura *et al*. (1989).

4. CONCLUSIONS

In this work, it was observed that the DNA Comet Assay and Half Embryo Test could detect the irradiated cells of lentils. In both cases, differences between irradiated and non-irradiated cells could easily be observed.

REFERENCES

1. LOAHARANU, P. (1994) Food irradiation in developing countries: A practical alternative. **IAEA Bulletin**, 36, pp 30-35.
2. DELINCÉE, H. and BOGNÁR, A. (1993). Effect of ionising radiation on the nutritional value legumes, *Bioavailability'93*. Nutritional, Chemical and Food Processing Implications of Nutrient Availability 2, pp 367-371.
3. CERDA, H., DELINCÉE, HAINE, H. AND RUPP, H. (1997). The DNA "Comet Assay" as a rapid screening technique to control irradiated food. **Mutation Res.**, 375, pp 167-181.
4. KAWAMURA, Y., UCHIYAMA, S. and SAITO, Y. (1998) A Half-Embryo test for identification of gamma-radiated Grapefruit. **Journal of Food Science**. 54, N° 2, pp. 397-382.
5. DELINCÉE, H., MARCHIONI, E. and HASSELMAN (1993) Changes in DNA for the detection of irradiated food. bcr information. **EUR 15012 EN**.
6. DELICÉE, H. (1996) DNA "Comet Assay" for rapid detection of irradiated food. **Acta Alimentaria**, 25, pp 319-321.

7. KHAN, H.M., DELINCÉE, H. (1998) Detection of irradiation treatment of foods using DNA "Comet Assay". **Radiat. Phys. Chem.** Vol. 52, N° 1-6, pp. 141-144.
8. VILLAVICENCIO, A. L. C. H.; MANCINI-FILHO, J. and DELINCÉE, H. (1998) Application of different techniques to identify the effects of irradiation on Brazilian beans after six months storage. **Radiat. Phys. Chem.** Vol. 52, N° 1-6, pp. 161-166.
9. KAWAMURA, Y., SUZUKI, S. UCHIYAMA and SAITO, Y. (1992) Germination test for identification of gamma-irradiated wheat, **Radiat. Phys. Chem.**, 40, pp 17-22.
10. FIFIELD, C.C.; GLUMBIC, C. and PEARSON (1967) Effects of gamma-irradiation on the biochemical storage and breadmaking properties of wheat. **Cereal Science Today**. N°6, pp. 253-261.
11. VILLAVICENCIO, A. L. C. H.; MANCINI-FILHO, J.; DELINCÉE, H. (1997) Utilization of half-embryo test to identify irradiated beans. **Boll. Chim. Farm.** Millan, Vol 136, N° 11, pp. 670-673.

CHROMATOGRAPHIC ANALYSIS OF IRRADIATED MEDICINAL HERBS:

RHAMNUS PURSHIANA D.C. AND PAULLINIA CUPANA KUNTH

P.M. Koseki *, P.R. Rela *· A.L. C. H. Villavicencio *

* Instituto de Pesquisas Energéticas e Nucleares - IPEN-CNEN/SP,
CTR – Centro de Tecnologia das Radiações,
Laboratório de Análise e Detecção de Alimentos,
São Paulo, Brazil.

Abstract. This paper present some comparisons about the influence of high doses of irradiation and biochemical compounds synthesized by plants as alkaloids and flavonoids. Since raw materials are often contaminated with pathogenic bacteria, they can also result in serious human illness. The microbial contamination in these raw plant materials is the issue of several studies, which propose appropriate techniques for the reduction of microorganisms. Whether the essential oils, tannins, flavonoids and alkaloids will be influenced by irradiation will be analyzed. The powdered and dehydrated herbs for and medical uses will be irradiated with electron beam applying doses of 10, 20 and 30 kGy. The botanical species investigated will be *Paullinia cupana Kunth* (popular name Guaraná) is largely cultivated in Brazil and to very used as energetic drink, and *Rhamus purshiana D.C.* despite the nutritional value, this vegetable has important medicinal proprieties as depurate and diuretic. The alterations in the active principles in the herbs following increasing doses of radiation will be analyzed employing various methods of extraction and chromatography.

1. INTRODUCTION

Over the past decades, interest in drugs derived from higher plants, especially the phytotherapeutic ones, has increases expressively. It is estimated that about 25% of all modern medicines are directly or indirectly derived higher plants [1].

Nowadays the interest is increasing; therefore the consumer attention to the medicinal active plants is growing. In spite of the great advances observed in modern medicine in recent decades, plants still make an important contribution to health care. Pharmacological composition of these plants, which may produce many reactions in the human body as well as in obesity, arterial tension, calmative and so on can be improved with irradiation process or not. Herbal drugs have been since ancient times as medicines for a treatment of a range of diseases. The rich Brazilian flora, represents more than 20% of the plant species know in the world as raw materials for pharmaceutical preparations [1, 2]. Since the last decade microbiological decontamination of medicinal herbs by irradiation has been carried out and presented in many scientific articles. The microbial contamination in these raw plant materials

*Corresponding author. IPEN-CNEN/SP, Centro de Tecnologia das Radiações - CTRD

Travessa R. Nº 400. Cidade Universitária. CEP: 05508-910, São Paulo, Brazil.

Fax: +55-11-3816-9186

E-mail: villavic@net.ipen.br (Anna Villavicencio), pmkoseki@net.ipen.br (Paula M.Koseki).

is the issue of several studies, which propose appropriate techniques for the reduction of microorganisms. The radiation process is known as safe for a large variety of products and applications. It is effective in the reduction of pathogenic microorganisms and in the extension of shelf life of the product [3]. One of these techniques is radiation processing by gamma source industrial plants [4]. Other is the utilisation of accelerators. In order to safeguard consumers, treatment by ionizing radiation is allowed now in Brazil to medicinal herbs and pharmaceutical products. The aim of our study is observe if flavonoids and alkaloids will be influenced by irradiation.

2. EXPERIMENTAL

Samples - Local herbs companies in São Paulo, Brazil, provided dehydrated samples of *Rhamnus purshiana* D.C. and *Paullinia cupana* Kunth.

Irradiation - The powdered samples were irradiated in on plastic package in a electron beam accelerator facility of Radiation Dynamics Inc., USA (E= 1,5 MeV, I=25mA, installed in IPEN São Paulo, Brazil. The irradiation doses were 10; 20 and 30 kGy at room temperature. The thickness of samples was less than 0,5 cm.

Sample analysis - Flavonoids and alkaloids analysis was performed in a Thin Layer Chromatography according to Wagner (1995)[5].

Spectrophotometry UV was performed in a Shimatzu apparatus in 200 – 400 nm. Dilution was 1/100.

3. RESULTS AND DISCUSSION

No alterations in the flavonoids and alkaloids, after irradiation treatment in these herbs were observed. Chromatographic analysis of the different extracts irradiated at increasing doses indicated that there were no great differences in the chemical constitution of the herbs. The extracts, do not present any change in the colour following increase the irradiation doses (results are similar in other herbs extracts) as showed in the absorption peaks (fig. 1 and fig.2). The samples showed similar curves, no changes in the chemical compounds were observed. Pharmacological activity of medicinal herbs has been found satisfactory after treatment by high doses radiation.

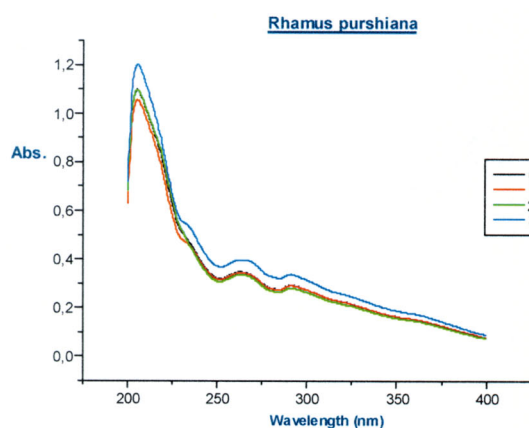


Figure 1 Absorption spectrum of *Rhamnus purshiana* extracts irradiated at different doses of radiation

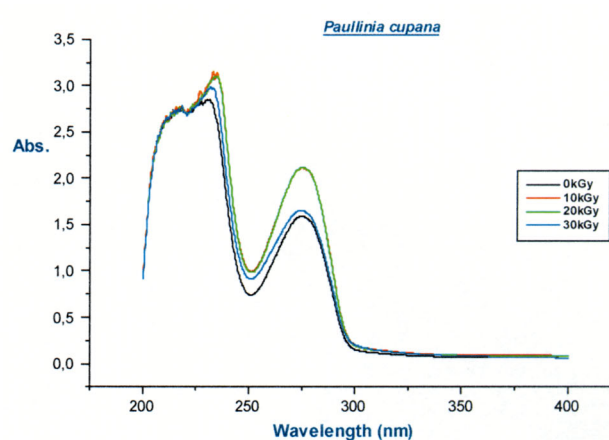


Figure 2: Absorption spectrum of *Paullinia cupana* Kunth extracts irradiated at different doses of radiation

4. CONCLUSION

Electron beams treatment carried out in this study, suggest that phytotherapies showed the identical therapeutically action as non-irradiated preparations after exposure to a dose of 10, 20 and 30kGy.

ACKNOWLEDGEMENTS

The authors are grateful to Quimer Medicinal Herbs –SP/ Brazil and IPEN/CNEN-SP.

REFERENCES

- [1] P.R.PETROVICK, L.C.MARQUES, I.C. DE PAULA, “New rules for phytopharmaceutical drug registration in Brazil ”; Journal of Ethnopharmacology 66 (1999) 51-55
- [2]. OLIVEIRA F, AKISUE G, AKISUE M. K, Farmacognosia. São Paulo: Atheneu; 1997
- [3]. RAZEM K.B, NOVAK B., RAZEM D. Microbiological decontamination of Botanical raw materials and corresponding pharmaceutical products by radiation. Radiation Physics and Chemistry, 2001.
- [4]. DELINCÉE H, MANCINI-FILHO J, VILLAVICENCIO A. L. C. H. Protein quality of irradiated Brazilian beans. Radiat. Phys. Chem, 1997.
- [5]. WAGNER, H. & BLADT, S. Plant Drug Analysis. A thin layer chromatography Atlas. Springer-Verlag. Berlin. p. 202, 230; 1995
- [6] Oliveira JED de, Marchini JS. Ciências Nutricionais. São Paulo: Sarvier; 1998.

INVESTIGATION OF DIRECT PRODUCTION OF ^{62}Cu RADIOISOTOPE AT LOW ENERGY MULTIPARTICLE ACCELERATOR FOR PET STUDIES

F. SZELECSÉNYI, Z. KOVÁCS

Cyclotron Department, Institute of Nuclear Research of the Hungarian Academy of Sciences (ATOMKI),
Debrecen, Hungary

K. SUZUKI, M. TAKEI, K. OKADA

Division of Advanced Technology for Medical Imaging, National Institute of Radiological Sciences (NIRS),
Chiba, Japan

Abstract. Excitation functions were measured by the stacked-foil technique for $^{59}\text{Co}(\alpha,n)^{62}\text{Cu}$ and $^{59}\text{Cu}(\alpha,2n)^{61}\text{Cu}$ nuclear reactions up to 45 MeV. The excitation functions were compared with published data. The optimum energy range for the production of radiocopper contamination free ^{62}Cu is 15→6 MeV. The calculated thick target saturation yield of ^{62}Cu in this energy interval was 9.34 mCi/μA at EOB (supposing three half-life [0.487 min] activation time). If <1% contamination level of ^{61}Cu is acceptable at the time of administration, the practical ^{62}Cu yield can be increased using higher bombarding energy. According to our calculations the optimum energy range for the production of ^{62}Cu was found to be 18.5→6 MeV. The calculated yield of ^{62}Cu in this energy window was 1.9 mCi/μA (16.2 mCi/μA at EOB) supposing 0.487 h irradiation and 0.5 h cooling times.

1. INTRODUCTION

There is a need for ^{62}Cu ($T_{1/2}=9.74$ min) PET radioisotope also in those laboratories where its generator (^{62}Zn [$T_{1/2}=9.2$ h]→ ^{62}Cu) are not available commercially and/or the ^{62}Zn can not be produced directly. The ^{62}Cu radionuclide is used mainly to label agents to quantify both blood flow and hypoxia [1].

In the past only one group studied a direct production way of ^{62}Cu (Piel *et al.* [2]). According to their results, this method resulted in very high production yield. Unfortunately this method requires highly enriched target material (^{62}Ni). The cost of the enriched target, the necessity of the recovery of the target material after the production, and the material loss during the irradiation/separation/recovery steps is a major disadvantage of this production way.

To avoid the use of highly enriched nickel target and the recovery problem, we have decided to investigate other production method(s) that do not employ enriched targets. Our candidate is the $^{59}\text{Co}(\alpha,n)$ reaction.

2. EXPERIMENTAL

To evaluate the optimum production circumstances of the ^{62}Cu via the above reaction and to solve the discrepancies exist among the literature cross-section results, excitation functions for the $^{59}\text{Co}(\alpha,xn)^{61,62}\text{Cu}$ nuclear processes were measured using the stacked-foil technique. Stacks of thin Co (thickness: 10 μm) and Cu (thickness: 9 μm) foils were irradiated with collimated alpha-particle beam from the AVF-930 isochronous cyclotron of NIRS, Chiba, Japan. The coppers foils served as energy degraders. The activation was performed with $E_{\alpha}=44.6\pm 0.5$ MeV alpha particles for 20 min using an integrated charge of 112.8 mC. The

stacks were placed in a cylindrical target holder acting also as a Faraday-cage. The radioactive decay of the residual nuclei in Co foils was followed without chemical separation using a Ge detector connected to an MCA operating on a PC. Since the ^{62}Cu has a very weak gamma line at 1173 keV, the annihilation peak was used for its identification. The cross-sections were calculated using the well-known activation formula. The combined uncertainty on the cross-sections was varied between 10 to 14%.

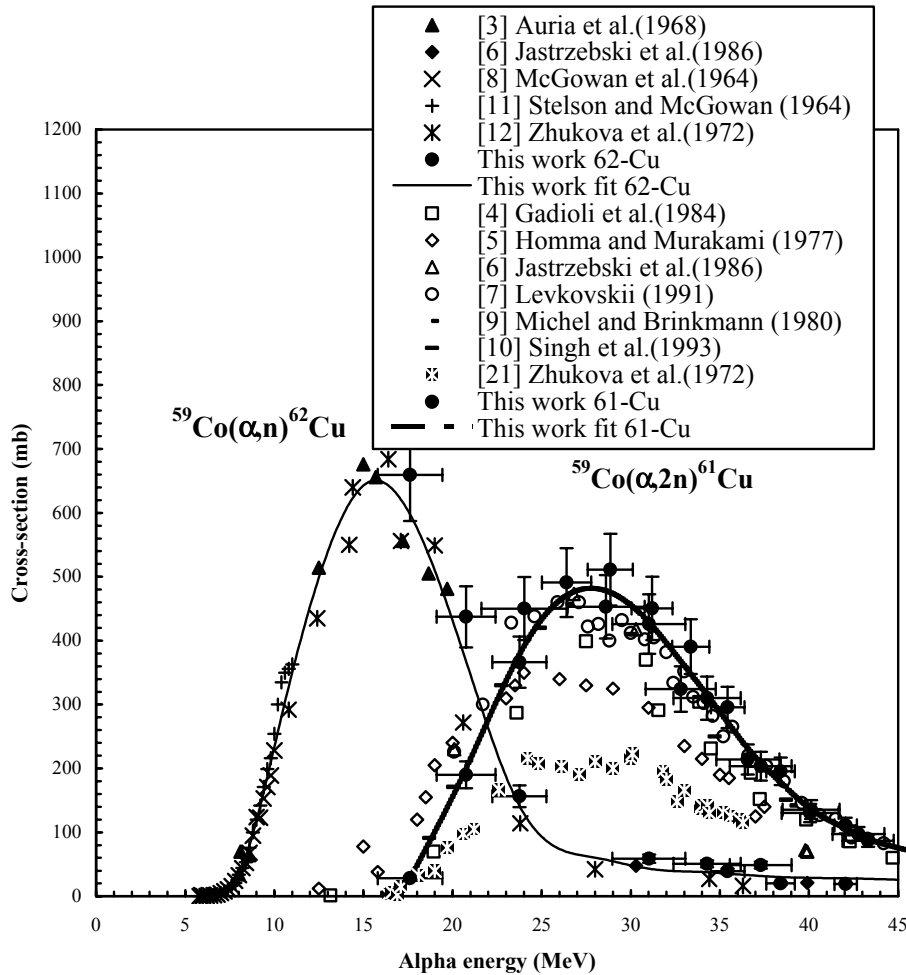


Fig.1. Cross-sections of $^{59}\text{Co}(\alpha, n)^{62}\text{Cu}$ and $^{59}\text{Co}(\alpha, 2n)^{61}\text{Cu}$ nuclear reactions.

3. RESULTS AND CONCLUSIONS

On the basis of the present measurement we have extended the database of the $^{59}\text{Co}(\alpha, n)^{62}\text{Cu}$ and $^{59}\text{Co}(\alpha, 2n)^{61}\text{Cu}$ nuclear reactions up to 45 MeV. The latter reaction forms the major contaminating copper radioisotope (^{61}Cu $T_{1/2} = 3.41$ h) during ^{62}Cu production. Our results together with the available literature values are reproduced in Fig.1.

As can be seen in Fig.1, our new values (9 cross-sections) agree well with the previous data in the overlapping energy regions. According to our work the excitation function curve of the $^{59}\text{Co}(\alpha, n)^{62}\text{Cu}$ nuclear reaction has a maximum of 650 mb (at 16 MeV). For ^{61}Cu , the measurement supports the data of those authors who reported higher values, and predict the maximum cross-section value at 28 MeV (around 490 mb). For yield calculations we have fitted all the acceptable cross-section results (including our present measurement) of the $^{59}\text{Co}(\alpha, n)^{62}\text{Cu}$ and $^{59}\text{Co}(\alpha, 2n)^{61}\text{Cu}$ reactions up to 45 MeV.

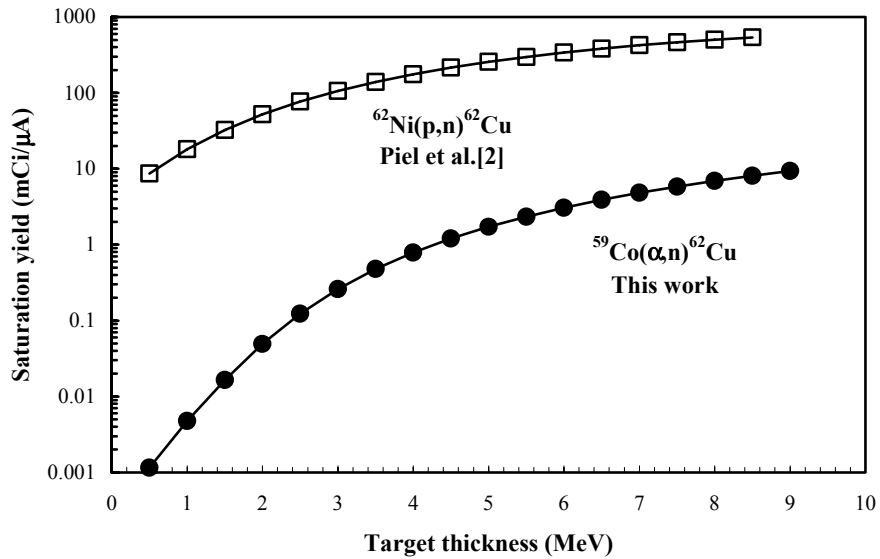


Fig.2. Saturation yields for the $^{62}\text{Ni}(p,n)^{62}\text{Cu}$ and $^{59}\text{Co}(\alpha,n)^{62}\text{Cu}$ nuclear reactions as a function of target thickness (target thickness: $E=E_{in}-6$ MeV).

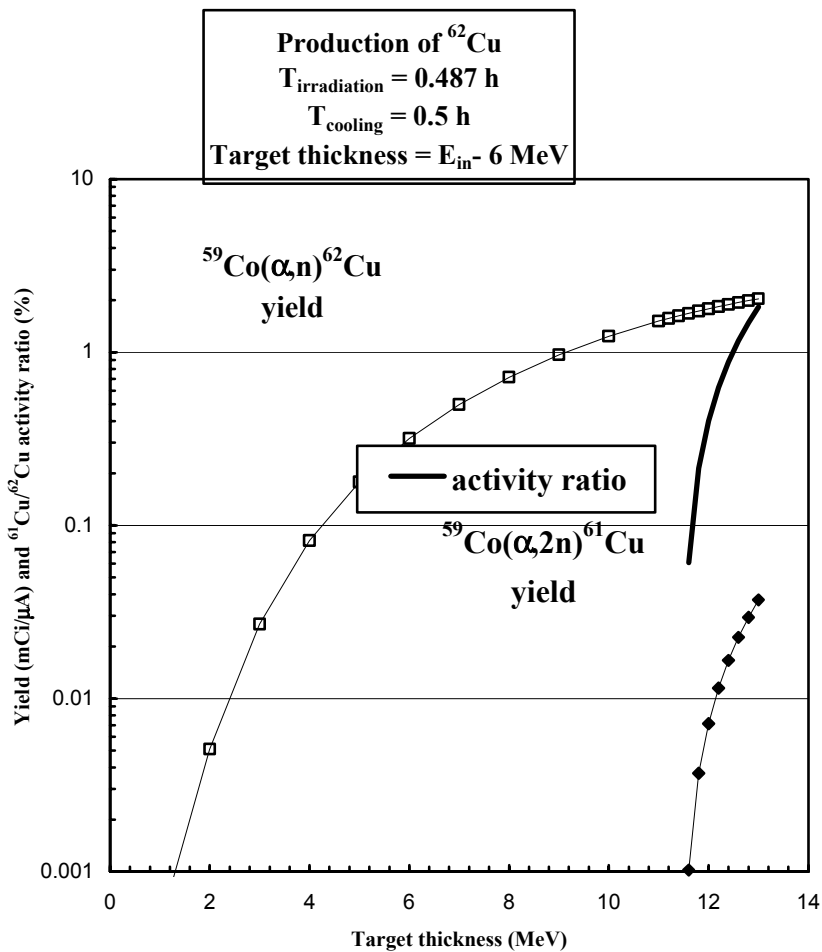


Fig.3. Practical yield of ^{62}Cu and ^{61}Cu and $^{61}\text{Cu}/^{62}\text{Cu}$ activity ratio as a function of target thickness ($=E_{in}-6$ MeV) (using 0.487 h irradiation time and 0.5 h cooling time).

The ^{62}Cu can be produced (see Fig.1) – without forming the longer lived ^{61}Cu - only below 15 MeV. According to our calculations the optimum energy range for the production of ^{62}Cu via the $^{59}\text{Co}(\alpha,n)$ reaction was found to be 15→6 MeV. The calculated saturation yield of ^{62}Cu in this energy interval was 9.34 mCi/ μA . We have compared in Fig.2, the ^{62}Cu yields using the $^{62}\text{Ni}(p,n)^{62}\text{Cu}$ [2] and $^{59}\text{Co}(\alpha,n)^{62}\text{Cu}$ nuclear reactions. Due to the expensive target material, Piel *et al.* [2] suggested a production energy window only from 14→10 MeV (328 mCi/ μA). This value is about 35 times higher than our yield, but taking into account the price of the enriched nickel and the problems of the recovery, the (α,n) production way could replace the (p,n) method for local ^{62}Cu production. Unfortunately, since a ‘minimal’ (approx. 0.5-1.0 h) processing time is still required after EOB (End of Bombardment) until the time of administration of the labelled compounds, any ‘practical yield’ (for both production ways) becomes much lower. However if <1% contamination level of ^{61}Cu is acceptable at the time of administration, and 0.5 h cooling time is enough for the ‘chemistry and labelling’, the practical yield can be increased using higher bombarding energy in the case of the $^{59}\text{Co}(\alpha,n)^{62}\text{Cu}$ reaction.

Fig.3 shows the available ^{62}Cu and ^{61}Cu practical yields (at three half-life [0.487 h] irradiation time and after 0.5 h processing time) as a function of target thickness. Additionally, we have reproduced the $^{61}\text{Cu}/^{62}\text{Cu}$ activity ratios (%) in this figure. According to our calculations the optimum energy range for the production of ^{62}Cu was found to be 18.5→6 MeV. The calculated yield of ^{62}Cu in this energy window was 1.9 mCi/ μA (16.2 mCi/ μA at EOB) and the level of ^{61}Cu is 1%.

As a result of this study it can be concluded that if the availability of a commercial generator is limited (like in our countries) even a low energy multiparticle cyclotron can be employed for in-house production of ^{62}Cu .

ACKNOWLEDGEMENTS

This work was done in the frame of a JSPS (Japan)-HAS (Hungary) bilateral Research Project ‘Development of new methods for targetry and synthesis of radiopharmaceuticals for research and applications in nuclear medicine’.

REFERENCES

- [1] FUJIBAYASHI Y., TANIUCHI H., YONEKURA Y., OHTANI H., KONISHI J., YOKOYAMA A., Copper-62-ATSM: A new hypoxia imaging agent with high membrane permeability and low redox potencial. *J. Nucl. Med.* **38** (1997) 1155.
- [2] PIEL H., QAIM S. M., STÖCKLIN G., Excitation functions of (p,xn) -reactions on ^{nat}Ni and highly enriched ^{62}Ni : Possibility of production of medically important radioisotope ^{62}Cu at a small cyclotron. *Radiochim. Acta* **57** (1992) 1.
- [3] D’AURIA J. M., FLUSS M. J., KOWALSKI L., MILLER J. M., Reaction cross section for low-energy alpha particles on ^{59}Co . *Phys. Rev.* **168** (1968) 1224.
- [4] GADIOLI E., GADIOLI ERBA E., ASHER J., PARKER D. J., Analysis of $^{59}\text{Co}(\alpha,pxn\alpha)$ reactions up to 170 MeV incident α energy. *Z. Phys.* **A317** (1984) 155.
- [5] HOMMA Y., MURAKAMI Y., Production of ^{61}Cu by alpha and ^3He bombardments on cobalt target. *Bull. Chem. Soc. of Japan* **50** (1977) 1251.
- [6] JASTRZĘBSKI J., SINGH P. P., MRÓZ T., VIGDOR S. E., FATYGA M., KARWOWSKI H. J., Interaction of 5-50 MeV/nucleon ^3He and ^4He with ^{59}Co . *Phys. Rev.* **C34** (1986) 60.

- [7] LEVKOVSKII N.N., "Middle Mass Nuclides ($A = 40-100$) Activation Cross Sections by Medium Energy ($E = 10-50$ MeV) Protons and Alpha-particles (Experiment and Systematics)." Inter-Vesi, Moscow, 1991.
- [8] MCGOWAN F. K., STELSON P. H., SMITH W. G., Cross section for the $Ni^{58}(\alpha,p)$, $Ni^{58}(\alpha,\gamma)$ and $Co^{59}(\alpha,n)$ reactions. Phys. Rev. **133** (1964) B907.
- [9] MICHEL R., BRINKMANN G., Alpha induced-reactions on cobalt. Nucl. Phys. **A338** (1980) 167.
- [10] SINGH N. L., AGRAVAL S., RAMA RAO J., Excitation function for α -particle induced reactions in light-mass nuclei. Can. J. Phys. **71** (1993) 115.
- [11] STELSON P.H., MCGOWAN F. K., Cross sections for (α,n) reactions for medium-weight nuclei. Phys. Rev. **133** (1964) B911.
- [12] ZHUKOVA O. A., KANASHEVICH V. I., LAPTEV S. V., CHRUSIN G. P., Nuclear reactions caused by α -particle on ^{59}Co nucleus. Yad. Fiz. **16** (1972) 242.

A COMPARATIVE STUDY ON PET AND SPECT IMAGE FORMATION SYSTEMS FOR A PROPER SCANNER CHOICE IN A CONSIDERED PET CENTER

G.R. Santos

Instituto de Engenharia Nuclear-CNEN, Rio de Janeiro, Brazil

A. de Oliveira, C. Luiz de Oliveira

Instituto Militar de Engenharia, Rio de Janeiro, Brazil

1. INTRODUCTION

In the last twenty years, the conjunction of technology and research had provided exceptional conditions for improvements on the quality of life, especially on nuclear medicine. In this area, the developed technology is being applied, making available better diagnoses and therapy to a variety of diseases. Since then the short-lived radionuclides were available only in the large physics research centers. The increasing clinical applications of radiopharmaceuticals have led to the rapid rise in the number of compact cyclotrons throughout the world. All medical cyclotrons currently available are suitable for sustaining programs for PET research and clinical application. To date, up to 122 medical cyclotrons have been established worldwide, and Brazil is about to install a new dedicated cyclotron (RDS111 from CTI), to its first PET Center, in Rio de Janeiro.

Also the number of scanners in use in the world has increased, mainly those based on the positrons emission and annihilation. The better result gotten in the final contrast of the object imposes necessarily a comparative study and analysis of the image formation process, either in a system based on a Single Photon Emission Computerized Tomography (SPECT), as well as on Positron Emission Tomography (PET.)

This comparative study should at least follow same increasing rates of the new devices with technological advances. That kind of study can be helpful on the decision of what type of scan should be the proper one, to a PET Center, on a specific region. Obviously, many other parameters are involved in that decision, and this discussion and analyses are the main subject of the present work. The objective is to make available a realistic comparative scenario, considering as many as possible the parameters involving.

Many of the new devices have been introduced making great progresses. As an example, in the new PET scanners, the reduction of examination time, and the remarkable improvement on the diagnoses based on images. As a consequence, we have a broadening on the field of application, better performance, and making possible the precocious discovery of males. Presently multi-ring commercial PET scanners can operate in either two or three-dimensional acquisition modes. Some special features like the lead septa positioned between the rings of detectors are retractable allowing 3-D acquisition. In this mode the overall scanner sensitivity has a remarkable increasing compared with earlier scanners, in spite of an increase in both the scatter and random rate.

Considering that all emission and transmission data are fed into the computers, and the coincidence events are stored as sinograms, it is also necessary to keep up with computational area. Just to give an idea on the complexity level, the software should be able to provide a full 2-D or 3-D reconstruction algorithm, based on filtered back projection, incorporating an attenuation

correction procedure. This is necessary to characterize sinograms, which correspond to sets of two-dimensional projections of the tracer distribution. Software tools should also have the capability for image manipulation and ultimately using various bio-mathematical models. This way, the PET data could be transformed into information with physiological, pathological significance. In addition, a full determination of the quantitative information requires a kinetic model of the transport mechanism and of the physiological and biochemical processes in which each radiopharmaceutical participates.

In a self-sustained project, like the PET Center's project in Rio de Janeiro intend to be, the most important parameters to be considered in the equipment's choice are the per capita's income and acquisition and maintenance costs. However, these factors by itself cannot predict which the best equipment should be acquired and some inherent characteristic of the product as resolution, sensitivity, time of resolution, time of scan and others capabilities should be considered.

Out of the comparative scenario regarding the relation cost-benefit, there are also some legal complies. Specifically connected to project of PET Center in Brazil, is the fact that the production of radioactive substances are monopoly of the federal government. As a consequence, and also considering that most PET radioisotopes are short-lived, the availability is restricted to this Southeastern region of Brazil. This region possesses technology to produce a large variety of radioisotopes/radiopharmaceuticals. That restriction also imposes another parameter related with regional disease that could be diagnosed by PET SPECT.

Beyond the previous facts, the proper dealing with scanners requires many others' capabilities. For instance, it is indispensable to understand all the internal equipment's details, knowing the process of image formation and analyses in PET/SPECT. This knowledge should cover the radioactive source preparation, the bombarding in a cyclotron, and the distribution and injection of the radiopharmaceuticals. Also in this knowledge is included the positron emission and annihilation, the types of radiopharmaceutical syntheses, the types of crystals, the influence of the collimators in the final image, the identification of the interaction point, the formation's principle of the plans and colors, the ways to introduce corrections, and to keep up with the new developments on the market.

As mentioned before, this is part of PET Center project in Rio de Janeiro, and this study is still being carried out, and the objective here is to present the current status of the study. This way, it will be presented next just a specific part related to the PET and SPECT scanners and associated equipment. Once finished, we intend that being presented to this work, the technologist must be able to evaluate and define a proper scanner, by established criteria. Following should also be able to make the choice and develop a protocol for its use. As a result of the proposed procedures, is expected a positive impact on the reduction of general costs and better quality of life reflected by a better diagnosis e a proper therapy.

2. BASIC COMPOSITION OF A NUCLEAR MEDICINE SCANNER

The complete equipment is basically composed of four elementary parts: radiation detection system, collimators, point identification system of radiation interaction, and computing system. The description of each one is presented with the objective of constructing the basis of a comparative framework.

2.1. Influence of the collimators in SPECT and PET

In any nuclear medicine equipment the collimators have a fundamental role, considering that they are close linked to the resolution and sensibility. The influence of the collimators varies with the scanner's operation mode. In the SPECT systems, or coincidence chambers (DHC), there is no acquisition mode without collimators usage. The collimator type is selected according the type of object under observation and the desired resolution. Also, it should be considered the type of radiation, high or low energy, that is being measured.

The collimators' usage in PET system has the objective a Field of Vision (FOV) reduction and to define the acquisition mode. There is two ways of getting PET images: 2D or 3D. In the 2D acquisition mode an axial lead shielding (septum), is inserted between each two detectors' ring, limiting the FOV and, this way, reducing the counting rate. This kind of application is frequently used for urinary bladder and brain studies. That kind of exam requires high radioisotopes doses, and consequently high counting rates. Also, the usage of septa reduces the spurious counting, allowing to speed up the processing, and improving resolution and final image quality.

When the axial shielding is not used one has the 3D acquisition mode. In that type of acquisition each detector in a ring can form coincidence lines with one detector of any other ring. The main advantage of that acquisition mode is the scanning time reduction and the radiopharmaceutical dose required for the exam. This will obviously reduce the patient dose. In the other hand, the increasing of FOV and counting rate can give rise to detection errors. That could be explained due to the increasing number of spurious events. Also, there will be a timing increase and imaging processing errors due to high volume of information to be processed, considering the need of more powerful reconstruction algorithm. Another immediate result of those facts is the resolution losses on the final imaging due to the increase in sensibility.

2.2. Radiation Detection System

There are several types of radiation detectors: gas, proportional, scintillation e semiconductors. The efficiency of each one of these detectors is related to different factors from which it could be emphasized that the most critical is the radiation type to be measured. In PET system is used scintillation detectors because they are more indicated the 511 keV gamma ray detector.

2.3. Point Interaction Localization System

The location of the point interaction in the crystal, where the annihilation occurs, must be determined with accuracy for better formation of the pictures. For this propose the nuclear medicine equipment (PET/SPECT) make use of the amount of light received for each fotomultiplier.

When the ray-x or gamma interacts with the crystal, light pulses are generated and are counted in the PMTs. Measuring the amount of light received for each one, and associating with the maximum amount that could be received, it is possible to determine, with accuracy, the place of radiation interaction. For that reason the scanners are equipped with a voltage divider. This divider is created from an electrical resistance composition and an intermediate key. The

principle is based on the fact of that the voltage and the loss of energy in an electrical resistor is proportional to the distance traveled by the electrons that are crossing the resistor. Therefore, for each key's location in the electrical resistor there will be a different voltage as a result. In this circuit each one of the pre-amplifiers is connected to the corresponding PMT. This way there will be four directing terminals X_+ , X_- , Y_+ and Y_- . These terminals represent Cartesian axes X and Y (positive and minus parts). The increase or reduction of the current pulse can be made by diminishing or magnifying, respectively, the distance of each photomultiplier to the terminal.

The ideal situation to have the accurate location of the radiation interaction point with the crystal, is to have a single block of crystal, as in SPECT. For this, it would be a transformation of the blocks in points. Therefore, if the system was ideal system, the accurate place would be easily determined. Unfortunately, this is not possible due to the fact of the amount of light received by each region, be dependence on the number of photomultiplier and its diameters. Thus, instead of getting the exact point, one gets the region of interaction.

As way to reduce this uncertainty area, the PET equipment, instead of using only one crystal, they make use of several blocks of small crystals detectors. Thus, the interaction region will be restricted to the crystal surface area. The light scattering process is directly connected on how is made the cuts in the crystals. In PETs, the cuts are made in a differentiated way, with the purpose to lead the light more accentuadamente to the vicinity region. With these techniques, the location of the crystal becomes easier and also speeding up the data processing. In these equipment the four crystals of the edges, figure 1, receive entire cuts. Between the cuts the crystals are painted with especial tints [7] serving as light guides. These tints diminish the refraction magnifying the reflection, making almost impossible the light scattering. For that reason when receiving the gamma ray interaction, the light produced in one of four crystals of the edges, all the light is restrained in it not passing to neighboring crystals (1A). The others cuts receive the same tint guide-of-light, but now in a partial way, allowing some light scattering to regions with no cut (figure 1B).

With this artifice, the amount of light received for each PMT will depend on each crystal has occurred the energy loss. This methodology is presented in Figure 1.

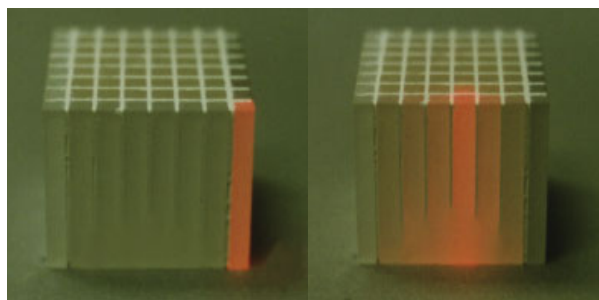


Figure 1: Light scattering due to the interaction near to the edging block, and due to the interaction near to the center block. In the illustration the crystals are made of bismuth germanate. The painted region is clear in both crystal blocks.

Making partial cuts, the passing of light from a crystal to another one becomes easily making possible the transference of light between the quadrants. This way, the amplitude of the responses peaks will be proportional to the amount of light contained in each crystal. Thus, a more precise point of interaction can be determined by eliminating the lesser intensity peaks. With this the peak of bigger amplitude will give the location of the crystal where the interaction has occurred. The interpretation of that processing is made through the Fourier transform [8].

2.4. Computing System

After receiving the signal of coincidence, registered by the electronic system of detention, various steps are executed by the systems of computers until getting the image of interest.

Considering a clinical system to be a set of protocols study, a system that automatically configures scanner for acquisition and processing becomes necessary. Using these protocols the operator would not need to enter with great amounts of data, the sweepings time, number of figures, reconstruction parameters and other that would be carried out automatically, giving much more speed to the system and preventing human fails. In special cases it is important granting to the operator the flexibility of choosing certain parameters as time of study and reconstruction parameters. Moreover, due the number of patients/day in a PET center, it is necessary a processing unit (CPU) for processing the previous acquired studies. The processing of the data is made by a work station that must be connected to a network to guarantee an intercommunication between the acquisition systems and processing and for the handling of the operator.

In a PET scanner the data are digitized and stored as matrix [3], either 64x64 or 128x128. So, each received pulse by the multichannel will have a specific location in the matrix. These arrays are divided into pixels, and are constructed in such away that they all cover the region of interest. Each one of the matrix cells carry information of one definitive region of the organ in study. This way, pixels can represent the number of counts registered in a specific point of the organ.

The data storage is made by the multichannel analyzer and is represented in the storage matrix through by the x, y coordinate (columns and strings, respectively). Each channel will be associated to one determined number of counts. These counts, in its turn, will be associated to a gray scale. Thus, the counts represented by each pixel can be represented as gray tones in accordance with the number of counts or number of points that represent them.

The data visualization is also made by representation through matrix (64x64, 128x128, 1024x1024 or even greater). The pixel size of a visualization matrix can change after the scan is finished. Despite of the pixel being able to vary in size, the visualization matrix size does not change. In this case what it is modified is the number of pixels of the matrix. Also, the system resolution does not change, making the point in the visualization matrix to change.

In a SPECT system, the size of pixel D , that cannot exceed $1/3$ of the width at half maximum (FWHM), is given by:

$$D = FOV/Z_n \quad (2)$$

where

FOV is the field of axial vision;
Z is the factor of zoom;
n is line number or columns;

3. PARAMETERS TO BE CONSIDERED WHEN CHOOSING PET/SPECT EQUIPMENT

There are many factors that must be taken in consideration for the selection of an equipment PET, SPECT or DHC. The five top reasons are: acquisition and maintenance cost of the equipment, price of specialized man power, per capita income of the potential patients and the capacity to diagnosis certain diseases. For the proper choice of equipment involving these five terms, its intrinsic features must be taken in consideration. On top of that, it should be made a study on the new developments of the market, and be able to differentiate between pretty image and a image that really brings technical information.

The latest advance in nuclear medicine is the combination of PET/SPECT with other devices, as the computerized tomography (CT), that is now forming the called hybrid devices. Also, is the progress in the methods of reconstruction [1, 9-10], correction of the images, and the crystal generation, the Luthercium oxioortosilicate (LSO)[11]. However, an image does not need, sometimes, to have a very great resolution to give a satisfactory diagnosis. Many times a SPECT with an adequate selection of filters can do the proper job. This way, knowing the real necessities of the region is a good start to determine which type of device must be acquired.

In Brazil, presently, the selection criteria receive an additional parameter that must be considered as the most important. That parameter is related to the fact that the basic supply for Scanner (radiopharmaceuticals) is under the federal monopoly. The consequence of that, and also considering that positron emitter radiopharmaceuticals are short life-time is very clear: the PET or DHC system is restricted only to the great centers¹ of the country, where are located the radioisotope production facilities.

For these regions this work is focused on determine which is the ideal equipment. To accomplish that, all mentioned factor should be considered. In this case the question to be addressed is if the area needs a PET or a SPECT for a scheduled study. Or still for regions where they are installed SPECTs, which is the best solution, buying a PET or to making an upgrade transforming into DHC is sufficient. For the rest of regions the work will be focussed in determine which type of SPECT that must be used.

REFERENCES

- [1] ZANG-HEE C, JOIE P. Jones & Manbir Singh *Foundations of Medical Imaging*, John Wiley & Sons Inc. (1993), ISBN 0-471-54573-2.
[2] FARR R.F. & ALLISY-ROBERTS P.J. *Physics for Medical Imaging*, W.B. Saunders Co. (1996), ISBN 0-702-01770-1

¹ Rio de Janeiro e São Paulo are the only Brazilian centers with technology to produce radioisotopes positrons emitter.

- [3] KENNETH R. C., *Digital Image Processing*, Prentice-Hall Inc., (1979), ISBN 0-13-212365-7.
- [4] JOHN BALL & ADRIAN D. M. *Essential Physics for Radiographers*, 3rd Ed., Blackwell Science (1997), ISBN 0-632-03902-7.
- [5] AIRD E.G.A. *Basic Physics for Medical Imaging*, Heinemann Medical Books (1988), ISBN: 0-750-61796-9.
- [6] STEWART BUSHONG C., *Radiological Science for Technologists. Physics, Biology and Protection*, 6th Ed., Mosby-Year Book (1997), ISBN 0-8151-1579-2.
- [7] INSTITUTE OF MED BOARD ON BIOBEHAVIORAL SCIENCES AND MENTAL DISORDERS, *Mathematics and Physics of Emerging Biomedical Imaging* National Academy Press (1996), ISBN: 0-309-05387-0
- [8] THOMAS R. N. & DOLORES H. P., Interactive Acquisition, Analysis and Visualization of Sonographic Volume Data, *International Journal of Imaging Systems and Technology*, **8** (1997), 26-37.

STATUS OF THE INSTALLATION OF THE AMS SYSTEM AT THE NUCLEAR REGULATORY AUTHORITY, IN ARGENTINA, DESIGN OF A NEW STRIPPER SYSTEM.

D.E. Alvarez, G.R. Bustos, A.J. Amodei, A.G. Bonino, M.A. Giannico, G.A. Serdeiro,
C.O. Rodríguez, C. Pomar
Autoridad Regulatoria Nuclear,
Buenos Aires, Argentina

Abstract. A new Accelerator Mass Spectrometer (AMS) system is under installation at the Nuclear Regulatory Authority, in Argentina. Its injection spectrometer is already operative, the electrostatic FN tandem accelerator is under high voltage test and the post accelerator spectrometer is been installed at present. A brief account on the status of the facility is presented. Results from preliminary test, for the design of a new terminal gas stripper system are presented.

1. INTRODUCTION

The main goal of the new Accelerator Mass Spectrometer (AMS) system [1], under installation at the Nuclear Regulatory Authority, is to perform AMS assays for actinides in the area of international safeguards, in particular safeguards related with ABACC⁺ and IAEA. A survey on the present status of the AMS technique, applied to actinide isotopes, can be found in ref. [2]. In the following section we describe the status of the facility. Finally the results of some preliminary test, oriented to the design of a new terminal gas stripper system are presented.

2. THE AMS SYSTEM

2.1 Injection Line

The layout of the entire system is shown in Fig.1. A high-current sputtering ion source provides negative ions of about 34 keV of energy. The emittance matching section consists in two Einzel lenses operating in telescope mode. Between them, a dog-leg steerer allows for minor alignment corrections.

A variable aperture is placed at the object focus of the 90°, 500 mm radius split-pole injection magnet (mass-energy product of 17.4 amu MeV). At its image focus are located the momentum defining slits, coincident with the object focus of the 90° spherical electrostatic analyzer, which has also a radius of 500 mm. Finally a third Einzel lens and another dog-leg steerer, match the beam into the accelerator.

Several tests have been done with sulfur and chlorine beams. The sample material was placed in copper holders having two different openings of 2 and 4 mm. The beam spot on the sample was usually between 0.5 and 0.7 mm in diameter. Currents between 10 and 12 μ A for ^{32}S and ^{35}Cl were measured at the image focus of the injection magnet. The transmission through the spherical electrostatic analyzer was 97% for both beams.

+ ABACC: Brazilian-Argentine Agency for Accounting and Control of Nuclear Materials

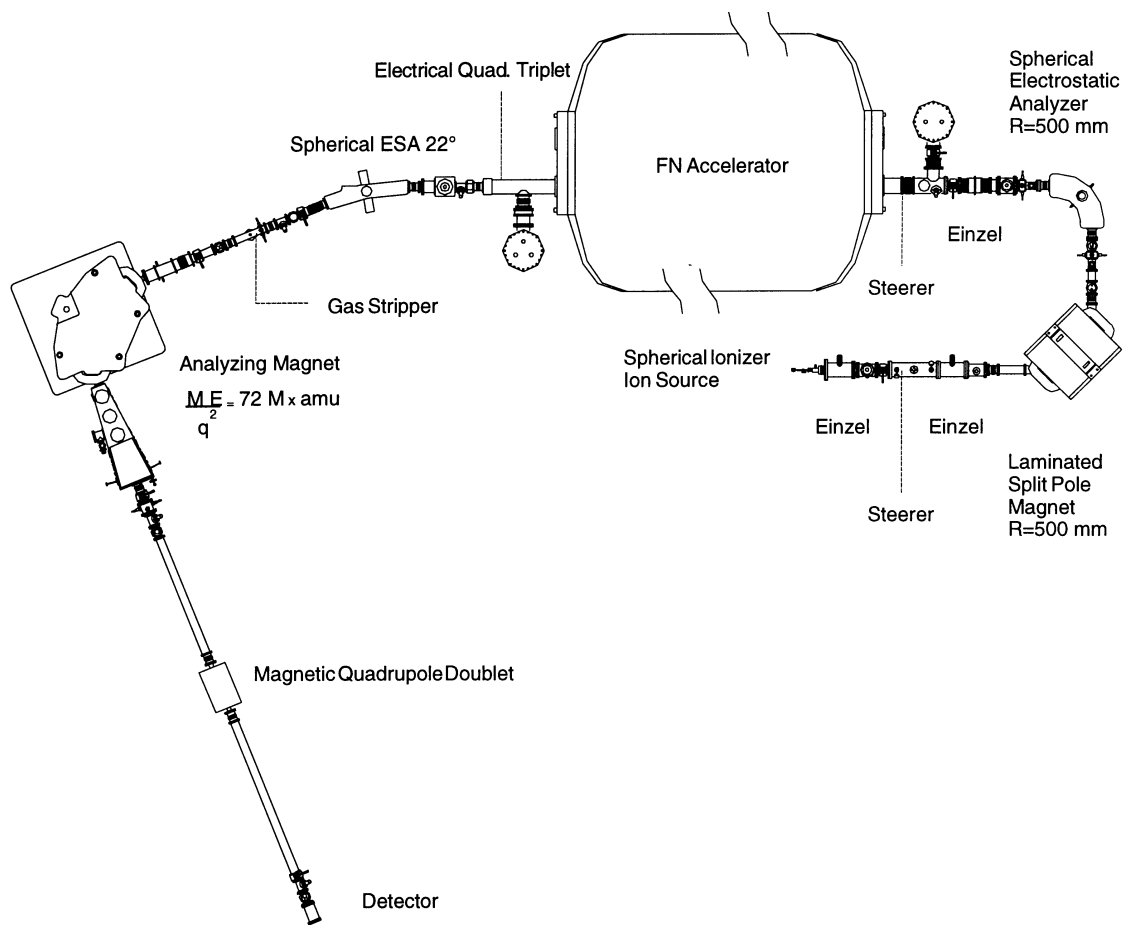


Fig. 1. Plan view of the AMS system.

2.2 The accelerator

The accelerator is a FN electrostatic tandem equipped with spiral inclined field acceleration tubes and a dual Pelletron charging system. Diamond-like stripping foils of $0.6 \mu\text{g}/\text{cm}^2$ (with supporting mesh) will be used at the terminal stripper in order to minimize energy and angular straggling when measuring actinide ions. With the same purpose, as will be discussed later, a new terminal gas stripper system is under study.

At the high-energy base of the accelerator tank, 22 cm downstream the exit of the last accelerator tube, an electric quadrupole triplet has been installed in order to keep the mass-independent tuning, along the complete system.

The isolating gas inside the pressure vessel is a standard mixture of N_2 plus 20 % CO_2 . The high voltage tests, without acceleration tubes, are under course at present.

2.3 The high-energy line

The electric quadrupole triplet at the high-energy base of the accelerator, followed by the 22° spherical electrical analyzer, focus the beam at the object of the analyzing magnet. At this position the beam charge state already selected by the electrical analyzer enter the external gas stripper. The main purpose of this second stripping is to increase the charge state of the beam in order to bent the actinide ions with the small 72 MeV x amu double focussing analyzing magnet. The momentum-analyzed ions are then focused at the detection chamber by mean of the magnetic quadrupole doublet, whose mass-dependent tuning is not yet relevant at this stage. Two pair of electrical deflecting plates at the entrance and exit of the analyzing magnet [3] will allow switching between close mass isotopes, keeping fixed the magnetic field.

3. ON THE DESIGN OF A NEW STRIPPER SYSTEM

3.1 Stripping process and angular straggling

The ion charge exchange, at the terminal stripper of a tandem accelerators, is a fundamental process in AMS because allows the elimination of the molecular background from the analyzed beam. Carbon foils with thickness ranging between 2 and 20 ug/cm² are commonly used as stripping media. When lower thickness is needed, a gas flowing in a narrow canal open in both sides is used. The theory of the charge exchanging processes has been discussed by Betz [4]. Extensive studies on charge-state distributions have been published [5,6].

Under normal conditions, the beam transmission through the accelerator depends basically on the stripping efficiency. For heavy ions like actinides the transmission is particularly affected by angular straggling at the stripping medium. To overcome this problem the thickness of the stripping media must be reduce to values only attainable using gas stripping. Calculations of ion multiple scattering, assuming screened Thomas-Fermi and Lenz-Jensen potentials [7] have been performed to estimate the angular straggling [8-9]. A particular calculation for uranium ions of 3 MeV, stripped by argon gas at the equilibrium charge exchanging density (1.E16 atoms/cm²), in a stripper canal 1 m long, indicate that a minimum diameter of 1.6 cm is needed in order to transmit 85 % of the beam [10].

Our gas stripper canal is 80 cm long, and 0.8 cm in diameter. Although the referred calculations suggest that reducing the gas thickness to pre-equilibrium densities, smaller diameters would be acceptable, we have considered relevant to study the possibility of increasing the diameter of our stripping canal.

3.2 Differential pumping

The preservation of the high vacuum at the acceleration tubes is very important for AMS in order to minimize beam loses as well as continuum energy background due to charge exchange interaction with the residual gas.

In order to increase the diameter of the stripping canal, while preserving the vacuum in the acceleration tubes, the introduction of differential pumping in the terminal, is very important. Since 1984, when for the first time a turbomolecular pump was used to recirculate the stripping gas at a tandem terminal [11] an increasing number of similar upgrading has been performed up to now [12-16].

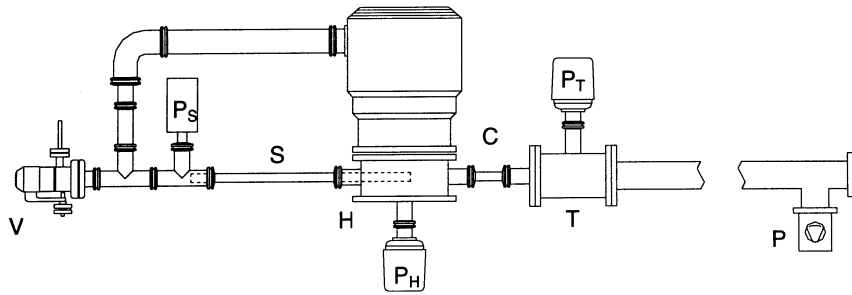


Fig. 2. Simple differential pumping system.

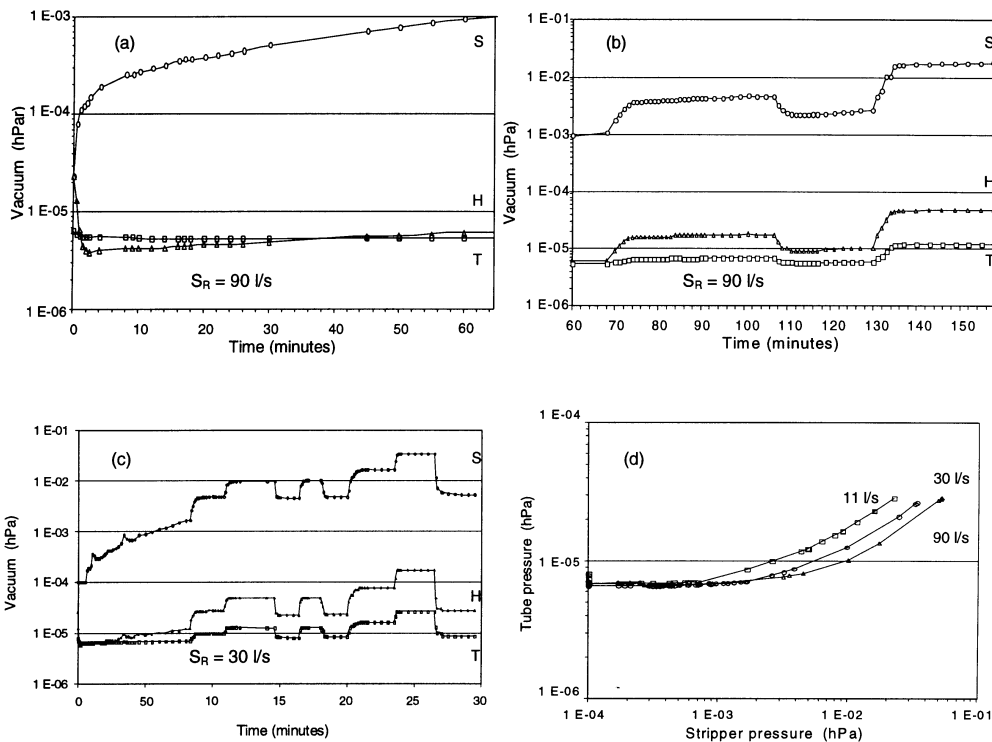


Fig 3. Time evolution of pressures at canal S, housing H and plenum T, (a) Recirculation speed 90 l/s and no nitrogen injection, (b) Recirculation speed 90 l/s, with injection of nitrogen, (c) Recirculation speed 30 l/s, without and with injection of nitrogen, (d) Trend of the high vacuum at plenum T when changing the as stripper pressure regime, for three different recirculation speeds.

Stripping of light ions like Be, C, Al, typically require carbon foils, in the range of 3 to 5 $\mu\text{g}/\text{cm}^2$. When using a gas, equivalent thickness in standard canal strippers is obtained with pressures in the range of 50-80 mTorr. But the gas pressure for stripping uranium ions, should not be greater than a few mTorr. In a recent AMS measurements for uranium with 3.5 MV at terminal, 5 mTorr at the stripper canal was reported [17].

In order to investigate the most relevant facts involved in the design of a gas recirculator that should operate with low pressures at the stripper canal we built the simple differential pumping system shown in Fig. 2. The turbomolecular pump, used to recirculate de gas, has a pumping speed of 500 l/s. Interposing

smaller apertures at its inlet port, the effective recirculation speed can be reduced. The stripper housing H has a volume of 1.1 liter. The turbo pump discharge is feedback to the stripping gas inlet with a tubing of 4.5 l/s conductance. The gas inlet valve V can inject nitrogen with controlled sensitivities as small as 1.0×10^{-10} Torr-l/s. The stripper canal S has a diameter of 1,6 cm and a length of 36 cm (1.25 l/s conductance). A 2.6 l/s conductance tube communicate the stripper housing with the simulated accelerator tube T. The 300 l/s diffusion pump at P, produce an effective pumping of 30 l/s at T.

The time evolution of the pressure at S and the vacuum at H and T, have been measured for different recirculation speed. As shown in Fig. 3(a) before switching on the turbo pump, at the equilibrium vacuum established by the diffusion pump P, the pressure at S and H are higher than at T. When the recirculation begins, the pressure at the stripper S increases due to the pumping effect on the stripper housing as well as on plenum T, through conductance C. The pressure at the stripper housing reach a minimum when the molecules dragged by the turbo pump are balanced by the incoming molecular flow from both, the stripper canal exit and conductance C. Subsequently the molecular flow driven through conductance C progressively increase the pressure at H until a new equilibrium is reached on term of pumping speed at the opposite sides of conductance C. Depending on the particular design of a recirculating system, the equilibrium pressure at the stripper canal (before injecting gas) may become too high, if very low pressure are needed.

At this stage, valve V was open in order to set a 5 mTorr recirculation pressure of nitrogen. As shown in fig. 3. (b) the pressure at S increased monotonically. The increasing rate diminished for higher pressure regimes. This result showing the physical interplay between the conductivity of the recirculation circuit, pressure and throughput, indicate that there is a minimum constant pressure, at the stripper canal, for a given conductivity and recirculation speed.

Reducing the effective speed of the turbo pump was possible to set low stripping pressure with excellent stability and repeatability as shown in fig. 3(c).

The present test has been performed at the lowest vacuum expected at the terminal of our accelerator. A less restrictive compromise between the pressure level at the stripper and a too high recirculation speed can be anticipated for higher vacuums at the accelerator tubes. Additional tests for different canal stripper diameters and also lower vacuums are planed.

4. SUMMARY

The injection line is already operative, the electrostatic FN tandem accelerator is under high voltage test and the high-energy line is been installed at present. After the accelerator tubes been installed, the measured vacuum at the terminal will be a critical information to perform more realistic gas stripper simulations.

REFERENCES

- [1] BENINSON, D., D' AMATTO, E., OLIVEIRA, A.A, STARK, J.W., BONINO, N.O., BUSTOS, G.R., ALVAREZ, A.E., AMODEI, A.J., BONINO, A.G., GIANNICO, M.A., and POMAR, C., Nucl. Instr. and Meth. B 172 (2000) 24.
- [2] FIFIELD, L.K., Nucl. Instr. and Meth. B 172 (2000) 134.
- [3] SIE, S.H., SIMS, D.A., NIKLAUS, T.R., and SUTER, G.F, Nucl. Instr. and Meth. B 172 (2000) 268-273

- [4] BETZ, H.D., Rev. Mod. Phys., 44 (1972) 465-539.
- [5] WITTKOWER, A.B. and BETZ, H.D., Atomic Data 5 (1973) 113-166
- [6] HOFMANN, H.J., BONANI, G., MORENZONI, E., NESSI, M., SUTER, M. And WOLFLI, W., Nucl. Instr. and Meth., B5 (1984) 254-258
- [7] SIGMUND, P. and WINTERBON, K.B., Nucl. Instr. and Meth. 119 (1974) 541.
- [8] SAYER, R., Rev. Phys. Appl. 12(1977) 1543
- [9] LITHERLAND, A.E., Iso Trace Report (1995) unpublished.
- [10] PURSER, K.H., KILIUS, L.R., LITHERLAND, A.E., and ZHAO, X., Nucl. Instr. and Meth. B 113 (1996) 445.
- [11] LEE, H.W., GALINDO-URIBARRI, A., CHANG, K.H., KILIUS, L.R. and LITHERLAND, A.E., Nucl. Instr. and Meth. B5 (1984) 208-210.
- [12] BONANI, G., EBERHARDT, P., HOFMANN, H.J., NIKLAUS, Th.R., SUTER, M., SYNAL, H.A. and WOLFLI, W., Nucl. Instr. and Meth. B 52 (1990) 338-344.
- [13] PURSER, K.H., ELMORE, D., MUELLER, K.A., MILLER, T.E., McK HYDER, H.R, and ENGE, H., Nucl. Instr. and Meth. B 92 (1994) 69-73
- [14] FALLON, J., WATT, G., JANE, S., RICE, D., and THORPE, K. pp 99-103
Symposium North Eastern Accelerator Personnel- 1995
- [15] HAKANSSON, K., and HELLBORG, R. Inter. Conf. on Heavy Ions Accel. Tech. Argonne National Laboratory, USA, 5-9 Oct. 1998, AIP Conf. Procs. 473 pp 94
- [16] JACOB, S.A.W., SUTER, M., SYNAL, H.-A., Nucl. Instr. and Meth. B 172 (2000) 235-24
- [17] FIFIELD, L.K., personal communication.

PRELIMINARY EXPLOITATION OF INDUSTRIAL FACILITY FOR FLUE GAS TREATMENT

A.G. Chmielewski, Z. Zimek, E. Iller, B. Tymiński,

Institute of Nuclear Chemistry and Technology, Warsaw, Poland

J. Licki

Institute of Atomic Energy, Świerk, Poland

Abstract. The experience gathered during laboratory and pilot plant tests has allowed for the preparation of the full scale industrial plant design. The electron dry scrubbing process was employed at the Pomorzany Electric Power Station - Szczecin in Poland for the simultaneous removal of SO₂ and NO_x from flue gases emitted by two Benson with a maximum flow rate 270 000 Nm³/h. Preliminary exploitation of industrial demonstration facility proved that SO₂ and NO_x desired pollutants removal efficiency from the flue gas can be obtained under certain conditions like sufficient humidity, suitable flue gas temperature, dose rate and ammonia stoichiometry.

1. INTRODUCTION

High emission of SO₂ and NO_x in the process of fossil fuel combustion creates a major world environmental problem. Poland which uses for energy production mainly pit and brown coal produces these pollutants as well. The certain amount of SO₂ and slightly less NO_x pollutants is introduced into the atmosphere. 1/2 of SO₂ and 1/3 NO_x pollution is contributed by heat and electricity generating boilers. The biggest sources of pollution are located in south west side of Poland and are connected with industrial centers but over 45% of the total SO₂ and 69% of NO_x pollutants distributed over polish territory come from external sources.

The laboratory facility for flue gas treatment radiation technology was organized in Institute of Nuclear Chemistry and Technology at Warsaw at the end of 80-ties. Soon after the pilot plant for flue gas treatment with electron beam has been installed at Power Plant Kaweczyn near Warsaw. The flow capacity trough those installations was respectively 400 and 20000 Nm³/h. Three new elements have been introduced to the construction of the radiation chamber in Polish pilot installation. Those are: cascade double stage irradiation, longitudinal irradiation, (beam scanned along the chamber axis) and the air blow under the chamber window with the purpose to create air curtain separating the window from the flue gases causing corrosion. Three different system for filtration aid has been constructed and tested: bag filter, gravel bead filter and electrostatic precipitator. The pilot plant installation was used to establish the optimal parameters of industrial facility:

- optimizing of the process parameters leading to reduction of energy with high efficiency of SO₂ and NO_x removal;
- selecting and testing filter devices and filtration process;
- developing of the monitoring and control systems at industrial plant for flue gas cleaning,
- preparation of the design for industrial scale facility.

The tests performed in the laboratory installations and the pilot plant resulted in the preparation of the industrial plant design. All the technical and economical analyses prove the advantages of this technology over present day conventional technologies.

2. INDUSTRIAL DEMONSTRATION FACILITY

The positive results of the tests performed on laboratory and pilot installation in Poland [1-12] has lead to decision concerning design and construction of the industrial demonstration plant for electron beam flue gas treatment. Industrial demonstration facility for electron beam flue gas treatment was designed and installed in EPS Pomorzany in Szczecin. This flue gas purification installation treats exhaust gases coming from a block which consists of two Benson type boilers of power 56 MWe each, supplying additional steam for heating purposes up to 40 MWth each. The 270 000 Nm³/h flue gases (half of produced by the blocks) is treated meet Polish regulations which are imposed since 1997.

Four electron accelerators has been constructed by Nissin High Voltage, Kyoto, Japan to provide 1200 kW of total beam power with nominal electron energy 0,8 MeV to be installed in EPS Pomorzany. Two-stage irradiation was applied as it was tested at the pilot plant. The industrial installation located at EPS Pomorzany consist of two independent reaction chambers, humidification tower with water and steam supply systems, ammonia water handling system with ammonia injection, electrostatic precipitator, by product handling system, measuring and control systems.

The flue gas is humidified up to 10% by volume in a dry bottom spray cooler. Ammonia is then injected before two parallel irradiation vessels. Longitudinal gas irradiation was applied (Kaweczyn pilot plant's solution). Formed aerosols are collected in dry ESP with a flat heated bottom furnished with a scraping device. Solid particles which are formed as salts are separated in ESP and byproduct pretreated in handling system with amount up to 700 kg/h.

The Pomorzany flue gas treatment installation has been designed for the station rated output reached after a retrofit of the plant. High concentration of NO_x and relatively low content of SO₂ in flue gas emitted from Benson boilers establish the specific conditions for flue gas treatment. The parameters of e-b process are chosen so as to guarantee efficiency of removal of NO_x up to 80% and of up 70% SO₂ in continuous operation of the installation. The main technical parameters and composition of flue gases in the Pomorzany e-beam installation are shown in Table 1.

All systems including accelerators were tested separately to meet EPS regulations (72 h continuos run) and confirm producer warranted parameters and facility design specification. Some necessary modifications including accelerators were introduced by equipment producers depends on obtained results of performed measurements. The quality of shielding properties of accelerator chamber walls was tested according to national regulation and the license on accelerator exploitation and personnel qualification were issued by polish authorities.

The spatial dose distribution and dose rate measurement were carried on with electron energy 700 and 800 keV. Preliminary results have shown that the construction solution of the reaction chamber (irradiation with scanning along the chamber axis and protective air curtain under the window to introduce the electron beam into the reaction chamber) approve themselves under industrial conditions. Calibration procedures of analytical equipment were applied to test instruments and obtain reliable data regarding facility running parameters. Experimental data obtained during preliminary exploitation show good agreement with results of theoretical calculations and performed pilot plant experiments.

Table 1. Technical parameters and composition of flue gases at key points of EB facility

Stream No.	1	2	3	4	5	6	7	8	9
	System gas inlet	Spray cooler outlet	Reaction chamber outlet	Process outlet	Spray water	Compressed air	Steam	NH ₃	By-product
N ₂	80 % vol.	75 % vol.	75 % vol.	75 % vol.					
O ₂	7 % vol.	6,6 % vol.	6,6 % vol.	6,6 % vol.					
CO ₂	8 % vol.	7,4 % vol.	7,4 % vol.	7,4 % vol.					
SO ₂	1,1 g/Nm ³	1,03 g/Nm ³	0,31 g/Nm ³	0,31 g/Nm ³					
NO _x	0,6 g/Nm ³	0,57 g/Nm ³	0,12 g/Nm ³	0,12 g/Nm ³					
NH ₃	0	0	0,03 g/Nm ³	0,03 g/Nm ³					
H ₂ O	5 % vol.	11 % vol.	11 % vol.	11 % vol.	11,1 t/h	3800 Nm ³ /h	4,5 t/h	180 kg/h	695 kg/h
(NH ₄) ₂ SO ₄	0	0	415 kg/h	0,012 g/Nm ³					
NH ₄ NO ₃	0	0	262 kg/h	0,007 g/Nm ³					
Solid particles	0,08 g/Nm ³	0,06 g/Nm ³	2,45 g/Nm ³	0,02 g/Nm ³					
Flue gas	270000 Nm ³ /h	284000 Nm ³ /h	284000 Nm ³ /h	284000 Nm ³ /h					

The primary task of preliminary exploitation is related to facility and separate systems optimization in respect to pollutants removal efficiency, energy consumption, by-product filtration efficiency, by-product handling system perfection, accelerator testing and improvement control systems perfection. The details procedures regarding facility operation were established to achieve smooth facility exploitation under typical conditions related to EPS service. The successful implementation of this technology in EPS Pomorzany may led to decisions concerning designing and construction other flue gas treatment facilities to solve environmental problems in Poland.

3. FINAL REMARKS

The results of the industrial facility preliminary exploitation indicate that:

- SO₂ and NO_x desired pollutants removal efficiency from the flue gas can be obtained under certain conditions like sufficient humidity, suitable flue gas temperature, dose rate and ammonia stoichiometry,
- depends on local conditions SO₂ or NO_x removal can be optimized to achieve primary goals of the installation,
- good reliability of the accelerators are the crucial for smooth exploitation of the facility,
- by-product quality may be influenced by coal and water quality used in the process.

References

1. CHMIELEWSKI, A.G., ILLER, E., ZIMEK, Z., AND LICKI, J. (1992) Laboratory and industrial research installations for electron beam flue gas treatment, *Applications of Isotopes and Radiation in Conservation of the Environment*, IAEA-SM-325/124, 81-92, Vienna.

2. ZIMEK, Z., CHMIELEWSKI, A.G., BULKA, S., LYSOV, G.W., ARTULAH, J.G., FRANK, N.W. (1995) Flue gas treatment by simultaneous use of electron beam and streams of microwave energy, *Radiat. Phys. Chem.*, 46(4-6), 1159-62.
3. CHMIELEWSKI, A.G., ZIMEK, Z., BULKA, S., LICKI, J., PIDERIT, G., VILANUEVA, L., AHUMADA, L. (1996) Electron beam treatment of flue gas with high content of SO₂, *Journal Adv. Oxid.*, 1(2), 142-149.
4. CHMIELEWSKI, A.G., ILLER, E., ZIMEK Z. AND LICKI J. (1992) Pilot plant for electron beam flue gas treatment, *Radiat. Phys. Chem.*, 40(4), 321-325.
5. CHMIELEWSKI, A.G., ZIMEK, Z., PANTA, P. AND DRABIK, W. (1995) The double window for electron beam injection into the flue gas process vessel, *Radiat. Phys. Chem.*, 45(6), 1029-33.
6. CHMIELEWSKI, A.G., TYMINSKI, B., LICKI, J. et al. (1995) Pilot plant for flue gas treatment - continuous operation tests, *Radiat. Phys. Chem.*, 46(4-6), 1067-1070.
7. LICKI, J., CHMIELEWSKI, A.G., ZAKRZEWSKA - TRZNADEL, G., FRANK, N.W. (1992) Monitoring and control system for an e-b flue gas treatment pilot plant-part I. Analytical system and methods, *Radiat. Phys. Chem.*, 40(4), 331-340.
8. LICKI, J., CHMIELEWSKI, A.G., RADZIO, B. (1995) Off-line system for measurement of nitrous oxide concentration in gases leaving the irradiation chamber, *Radiat. Phys. Chem.*, 45(6), 1035-38.
9. CHMIELEWSKI, A.G., LICKI, J., DOBROWOLSKI, A., TYMIŃSKI, B., ILLER, E., ZIMEK, Z. (1995) Optimization of energy consumption for NO_x removal in multistage gas irradiation process, *Radiat. Phys. Chem.*, 45(6), 1077-79.
10. CHMIELEWSKI, A.G., TYMINSKI, B., DOBROWOLSKI, A. et al. (1998) Influence of gas flow patterns on NO_x removal efficiency, *Radiat. Phys. Chem.*, 5(1-6), 339-343.
11. CHMIELEWSKI, A.G., ILLER, E., ZIMEK, Z., et al. (1995) Industrial demonstration plant for electron beam flue gas treatment, *Radiat. Phys. Chem.*, 46(4-6), 1063-1066.
12. CHMIELEWSKI, A.G., ILLER, E., FRANK, N.W. (1998) Technical and economic aspects of electron-beam installations for treatment of flue gases from power plants, IAEA-TECDOC, *Radiation Technology for Conservation of the Environment*, p.133-143.

CONTROL SYSTEM OF THE FOLDED TANDEM ACCELERATOR AT BARC

M.J. KANSARA, P. SAPNA, N.B.V. SUBRAHMANYAM, J.P. BHATT,
S.K. SINGH, P. SINGH
Nuclear Physics Division, Bhabha Atomic Research Centre, Mumbai, India.

T.S. ANANTHAKRISHNAN, M.D. GHODGAONKAR
Electronics Division, Bhabha Atomic Research Centre, Mumbai, India

Abstract. The control system of the Folded Tandem Ion Accelerator (FOTIA) at BARC, Mumbai India is described and the most important parameters are given.

Different site-specific approaches are followed by accelerator laboratories, to develop control systems. The requirements for the Folded Tandem Ion Accelerator (FOTIA) [1] control system at BARC are that it should be upgradeable, scaleable and simple to maintain. Incorporating these requirements, we have developed control architecture (hardware as well as software), fibre optic data telemetry system [2], spark protection circuit and the hardware interface units.

In FOTIA, the parameters of devices at various locations are controlled and monitored remotely using a computer based control system. The control system (Fig.1) has been developed with PCs forming the different nodes, connected through an Ethernet with CAMAC as front-end system. PCs are used as consoles and servers. FOTIA parameters are monitored and controlled through PC3, which includes a CC8 CAMAC controller PC interface card. This interface card communicates with the CAMAC controllers with System Interconnect Bus (SIB). CAMAC consists of a crate controller, data display and different plug in modules for Analog as well as Digital signals. Scanning rate of the system is 1 ms and refreshing rate is 1 sec. The operating system is QNX. Graphical application is implemented in C++. Communication, run-time database and objects are supported by the control system platform. Both QNX operating system and CAMAC have been tested and proven to meet the needs of FOTIA.

The various CAMAC modules like, Parallel Crate Controller with PC interface card, 16 channel scanning 12 bit ADC, 8 channel 12 bit DAC, 24 bit isolated input, 24 bit isolated output, multi channel serial communication module used in the control system for FOTIA, were developed in the Electronics Division of BARC.

For interfacing various power supplies with CAMAC, number of hardware interface modules were developed in house. A fibre optic data telemetry system was developed for control of the devices located in the high voltage environment. In order to get higher resolution required for controlling the magnet power supply, multi-channel serial communication CAMAC module is used.

A large EMI burst from the accelerator and ion source sparks can induce spikes in the power line and control system. A spark protection circuit for the protection of control system components was used. All the electronic gadgets and interface modules located in the high voltage terminal were shielded for EMI.

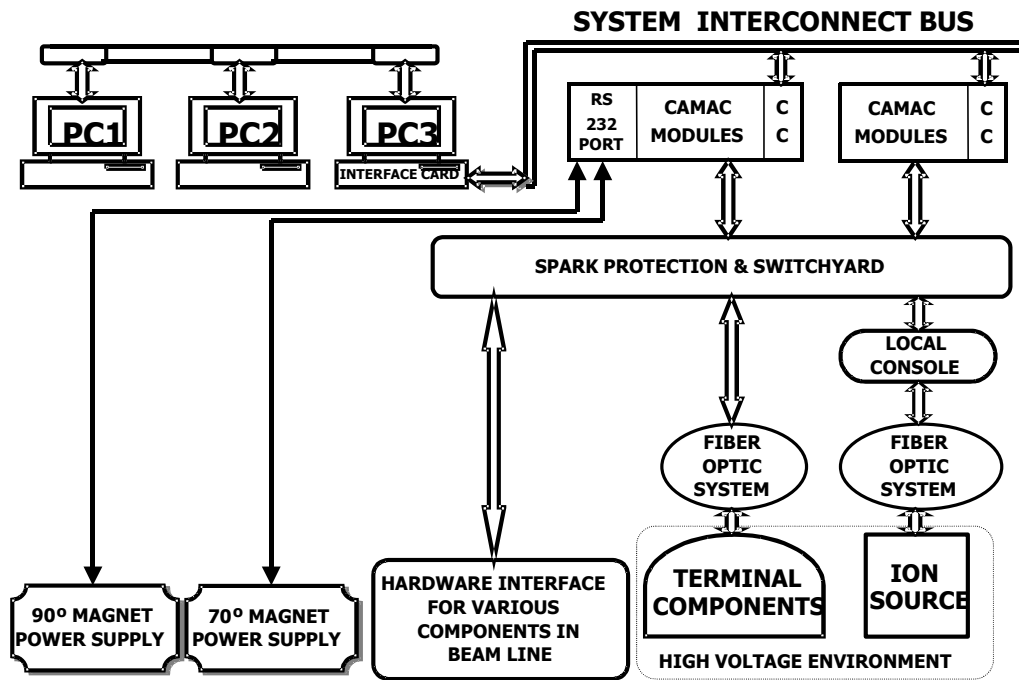


Fig. 1.

The operator interface has been developed using QNX windows. The operator can interact with the system using keyboard and mouse. The operator can change the parameter of device by selecting menu item and then clicking on buttons for the operation with minimum efforts.

This control system has been operational and extensively used during high voltage tests and beam trials. Its performance has been found satisfactory.

REFERENCES

- [1] SINGH P., Ind. J. Pure & Applied Phys. 35, 172 (1997)
- [2] KANSARA M.J. et al., Ind. J. Pure & Applied Phys. 35, 212 (1997)